http://esajournals.onlinelibrary.wiley.com/doi/10.1002/eap.70011: Williams, T., C. N. Janousek, M. A. McKeon, H. L. Diefenderfer, C. E. Cornu, A. B. Borde, J. Apple, L. S. Brophy, M. Norwood, M. A. Schulz, and S. D. Bridgham. 2025. Methane and nitrous oxide fluxes from reference, restored, and disturbed estuarine wetlands in Pacific Northwest, USA. Ecological Applications 35(2): e70011.

Methane and nitrous oxide fluxes from reference, restored, and disturbed estuarine wetlands in Pacific Northwest, USA

Trevor Williams[1], Christopher N. Janousek[1], Maggie A. McKeon[2], Heida L. Diefenderfer[2], Craig E. Cornu[3], Amy B. Borde[4], Jude Apple[5], Laura S. Brophy[3], Matthew Norwood[2], Matthew A. Schultz[6], Scott D. Bridgham[6*]

1. Department of Fisheries, Wildlife and Conservation Sciences, Oregon State University, Corvallis, OR 97331, USA

2. Pacific Northwest National Laboratory, Sequim, WA, USA

3. Estuary Technical Group, Institute for Applied Ecology, Corvallis, OR, USA

4. Columbia Land Trust, Vancouver, WA, USA

5. Padilla Bay National Estuarine Research Reserve, Washington State Department of Ecology, Mt. Vernon, WA, USA

6. Institute of Ecology and Evolution, University of Oregon, Eugene, OR, USA

* Corresponding author: bridgham@uoregon.edu

ORCID

Trevor Williams: 0009-0002-0417-3235
Christopher Janousek: 0000-0003-2124-6715
Maggie McKeon: 0009-0006-7908-9619
Heida Diefenderfer: 0000-0001-6153-4565
Craig Cornu: 0009-0001-1078-7762
Amy Borde: 0000-0002-5603-2832
Jude Apple: 0009-0000-0263-1015
Laura Brophy: 0000-0002-0485-5597
Matt Norwood: 0000-0001-8582-214X
Matthew Schultz: 0000-0001-5103-4305
Scott Bridgham: 0000-0003-0614-2678

OPEN RESEARCH

Data (Janousek et al., 2025) are available in the Smithsonian Environmental Research Center's repository at https://doi.org/10.25573/serc.27161883.v1.

FUNDING INFORMATION

The Effects of Sea Level Rise Program, Grant/Award Number: NA19NOS4780176; National Estuarine Research Reserve System Science Collaborative, Grant/Award Number: NA19NOS4190058

Keywords: boosted regression trees; estuaries; methane; natural climate solutions; nitrous oxide; restoration; tidal marsh; tidal swamp

Abstract

There is substantial interest in restoring tidal wetlands because of their high rates of long-term soil carbon sequestration and other valued ecosystem services. However, these wetlands are sometimes net sources of greenhouse gases (GHG) that may offset their climate cooling potential. GHG fluxes vary widely within and across tidal wetlands, so it is essential to better understand how key environmental drivers, and importantly, land management, affect GHG dynamics. We measured methane (CH_4) and nitrous oxide (N_2O) fluxes at 26 reference and restored tidal wetland sites and eight non-tidal pastures (mostly diked former tidal wetlands) in five estuaries in the Pacific Northwest (PNW), USA. We measured fluxes 7-8 times over one year to assess the effects of environmental drivers, wetland type, and land management on CH_4 and N_2O fluxes. Linear relationships between CH_4 fluxes and environmental drivers were poor, but a machine-learning approach with boosted regression trees provided strong predictability for fluxes based upon wetland surface elevation, water-table level, and salinity. Less important variables were groundwater pH, wetland type, and temperature. Under oligohaline conditions, CH_4 fluxes were variable and sometimes very high, but fluxes at salinities above 2 ppt were relatively low on an annual basis. Fluxes of CH_4 were higher in restored tidal marshes and wet pastures than in reference tidal marshes, tidal swamps, and dry pastures. The N_2O model had lower predictive power than the CH_4 model, with wetland type as the most important factor, though N_2O fluxes across all wetland types were low (median of zero). Our results indicate that estuarine hydrologic gradients are a key driver of CH_4 fluxes and that wetland land use impacts on CH_4 fluxes are largely mediated by their varying environmental conditions. In the PNW, estuarine wetlands that have low salinity, lower elevation, and have high water tables are more

likely to have increased CH_4 emissions that may offset their carbon sequestration benefits until they gain enough elevation through accretion. This study also provides a transferrable modeling approach to predict the consequences of coastal wetland management to GHG fluxes using monitoring data from a limited set of key environmental drivers.

INTRODUCTION

Global efforts to find natural adaptive solutions to help mitigate anthropogenic climate change have increased attention on coastal tidal wetlands, including emergent marshes, seagrass meadows, mangrove forests, and temperate tidal swamps, because of their ability to remove and store carbon dioxide effectively (McLeod et al., 2011). These “blue carbon” ecosystems are highly efficient, on a per-unit-area rate basis, at sequestering organic carbon derived from both *in situ* photosynthetic production and allochthonous carbon inputs from coastal watersheds (Chmura et al., 2003; Hopkinson et al., 2012; Peck et al., 2020; Kauffman et al., 2020; Poppe and Rybczyk, 2021). Interest in blue carbon has led to growing incentives for governments and land managers to conserve and restore tidal wetlands over the past decade (Kelleway et al., 2020), actions which have the added benefits of increasing habitat for fish and wildlife, providing flood protection, and sustaining the important cultural and biodiversity services of estuaries (David et al., 2014; Himes-Cornell et al., 2018).

Although blue carbon ecosystems have a high capacity to sequester organic carbon, they also can emit the powerful greenhouse gases (GHGs) methane (CH_4) and nitrous oxide (N_2O), potentially offsetting their cooling potential. Saline and brackish tidal wetlands are estimated to emit globally 0.76 Tg CH_4 yr^{-1} with much smaller emissions of 6.3 Gg N_2O yr^{-1}, but these GHG emissions are offset by soil carbon sequestration, so there is an estimated global net removal of 538 Tg CO_2 eq. yr^{-1} using a 20-yr global warming potential (Rosentreter et al., 2023). However, the range of GHG emissions observed both globally and regionally is large because CH_4 and N_2O production in wetlands is affected by a number of drivers conferring high heterogeneity in time and space (Hemes et al., 2018; Rosentreter et al., 2021; Capocci and Vargas, 2022). Global wetland CH_4 emissions also may have increased over the last two decades due to feedback from increasing air temperatures and precipitation (Zhang et al., 2023). It is important to understand how coastal land management affects GHG fluxes in estuarine wetlands because perceived positive climate forcing benefits may be a motivating factor in new restoration projects. Understanding how CH_4 and N_2O fluxes differ along key estuarine environmental gradients and among different management histories is crucial for determining to what extent these ecosystems can contribute to a suite of natural climate solutions that help mitigate global warming.

Variability in estuarine biogeophysical conditions influences CH_4 fluxes in tidal wetlands, with water-table level, salinity, and temperature being major factors (Tan et al., 2020; Rosentreter et al., 2021; Schultz et al., 2023). Low salinity wetlands emit higher and more variable levels of CH_4 (Poffenbarger et al., 2011; Sanders-DeMott et al., 2022), and 18 ppt (about half the concentration of seawater) is often used as a threshold between high- and low-emission tidal wetlands (IPCC 2014). Controls on CH_4 fluxes at lower salinities are more complex and involve multiple environmental drivers that may be non-linear and interact with one another (Schultz et al., 2023). New modeling techniques such as machine-learning approaches that account for non-linear and interactive effects of multiple environmental drivers can help researchers better predict GHG fluxes when there are potentially complex controls operating at multiple spatial and temporal scales (Yuan et al., 2022; Schultz et al., 2023).

Two recent meta-analyses found disparate results regarding the effects of coastal wetland conversion to other land uses, and subsequent restoration, on CH_4 and N_2O fluxes (O’Connor et al., 2020; Tan et al., 2020). This emphasizes the need for further studies. Along the U.S. west coast, many tidal wetlands were historically diked, drained, and converted to agricultural uses, resulting in high levels of wetland loss and fragmentation of estuarine landscapes (Brophy et al., 2019; Marcoe and Pilson, 2017). To reverse loss and enhance estuarine function, efforts to restore tidal wetlands, particularly emergent marshes, are increasing all along the U.S. west coast. From a blue carbon perspective, it is crucial to understand how land management practices such as diking and subsequent draining and seasonal drying of tidal wetland soils may contribute to changes in CH_4 and N_2O production to inform accurate assessment of the overall climate effects of wetland conservation and restoration. Moreover, it is necessary to determine how GHG fluxes may change in restored sites over longer time scales as site conditions such as hydrology evolve. However, very little data exists on GHG fluxes in natural, disturbed, or restored tidal wetlands in the Pacific Northwest (PNW) region of the U.S. (Diefenderfer et al., 2018a; RoyChowdhury et al., 2018; Schulz et al., 2023).

We conducted a regional assessment of CH_4 and N_2O fluxes from tidal wetlands across a range of land management regimes and wetland types in the PNW using a machine-learning approach to examine the relative impacts of environmental drivers on fluxes and to predict annual fluxes at the site level. Our study builds on more localized research in the region using a similar approach (Schultz et al., 2023). We measured GHG fluxes in least-disturbed reference tidal marshes and swamps, restored tidal marshes, and non-tidal pastures (mainly former tidal wetlands historically converted to agricultural land uses). At the same sites, we also measured environmental factors likely to affect fluxes, including water-table level, groundwater salinity and pH, soil and air temperature, and plant biomass and species composition. This study tested the following hypotheses: (1) CH_4 fluxes increase with greater waterlogging, lower salinity, and higher soil and air temperatures. (2) CH_4 trends related to environmental drivers are non-linear and interactive. (3) Plant biomass and community composition affect GHG fluxes. (4) CH_4 fluxes differ among estuarine wetland types and land management regimes, which can largely be explained by their effects on ecosystem drivers of these fluxes. (5) N_2O fluxes are low overall but are somewhat higher in former tidal wetlands now used for agriculture. By incorporating a large regional dataset into a machine learning model, we developed a framework that can be applied to estimating fluxes from other estuarine wetlands in the region where flux data are not available.

MATERIALS AND METHODS

Study sites

We measured GHG fluxes at 34 sites in estuaries on the Oregon and Washington coasts 7-8 times from spring 2021 to spring 2022, which differed in dominant vegetation, disturbance status, tide range, and salinity. Sites were located in the Coos Estuary (OR), Columbia River Estuary (OR/WA), Grays Harbor Estuary (WA), Skagit Estuary (WA), and Padilla Bay (WA) (Fig. 1A; Appendix 1: Table S1). Sites included 12 reference marshes, five forested tidal swamps, nine restored marshes, and eight non-tidal pastures. The nine restored sites ranged in age from about 5 to 25 years at the time of sampling, and were mostly dike breaches or removals to restore tidal connectivity. Tidal sites occurred across a broad continuum of salinity from tidal freshwater marshes and swamps in the Columbia River and Skagit estuaries (0-0.5 ppt) to oligohaline (0.5-5 ppt), mesohaline (5-18 ppt), and polyhaline conditions (18-30 ppt) in other estuaries. Marshes were dominated by a mixture of mostly perennial grasses, sedges, and forbs, while tidal swamps were dominated by trees (mainly *Picea sitchensis*) with woody and herbaceous understories. Pastures were non-tidal sites dominated by graminoid emergent vegetation and included six diked former tidal wetlands (two were being agriculturally managed and four were not at the time of sampling) and two in a coastal floodplain adjacent to estuarine wetlands but at elevations mostly above tidal influence. We classified three pastures as “wet pastures” (median water table 25 cm below the surface or higher for at least five months out of the year) and the other five sites as “dry pastures”. We combined wetland types and land management classes into a single class termed “wetland type” for brevity.

Gas sampling

At each site we inserted six PVC collars (40 cm diameter, 16 cm height) about 9 cm into the ground for the duration of the study. Drainage ports were inserted when necessary to facilitate drainage. Collars were situated at both ends of 2.4 m long wood boardwalks which were used to minimize sediment disturbance near the collars during sampling (Fig. 1B). At most sites, the three boardwalks were arranged along a short transect perpendicular to a major tidal slough (or ditch or stream in the case of non-tidal pastures) in order to capture gradients within sites due to differences in elevation, hydrology, and plant composition. At tidal swamp sites, because of the complex physical structure caused by tree roots and stumps, we installed the boardwalks in relatively flat areas.

At the time of sampling, we fitted collars with one or more 0.04 m^3 chamber tops (multiple top sections were stacked to accommodate tall vegetation) constructed from a PVC frame and 6 mil (i.e., 0.152 mm thickness) translucent greenhouse plastic affixed with clear adhesive tape to form an airtight seal. We drilled an intake port at the top and a return port at the bottom, installed with Swagelok fixtures, and connected to tubing which ran to the gas analyzer creating a closed loop system. Given the large number of widely dispersed sites, two teams were responsible for gas measurements, and a comparison of the two instruments gave similar slopes for CH_4 fluxes. We sampled the southern estuaries (Coos Bay and Columbia River) with a portable Fourier-transform infrared (FTIR) gas analyzer, Gasmet DX4040 (Vantaa, Finland), and the northern estuaries (Grays Harbor, Skagit, Padilla Bay) with an Optical Feedback – Cavity Enhanced Absorption Spectroscopy (OF-CEAS) gas analyzer, LI-7810 (LI-COR, Lincoln, NE, USA) (Fig. 1B). Only the Gasmet allowed for N_2O flux measurements. The Gasmet was out of service for several months, during which time we used the LI-7810 on all sites. Since N_2O sampling was limited to sites and months when the Gasmet was operational, the data set has about a third as many measurements as CH_4.

Battery operated fans placed inside the chambers mixed the headspace. We conducted light and dark measurements sequentially at each chamber to determine if light availability affected fluxes. We determined dark fluxes by placing black plastic sheeting over the chamber tops and measuring gas concentrations for approximately 6 min. We then removed chamber tops, allowed gas concentrations to return to ambient levels, and replaced chamber tops for light measurements for another 6 min. The LI-COR sampled continuously at about 1 hz and the Gasmet samples were averaged every 30 s.

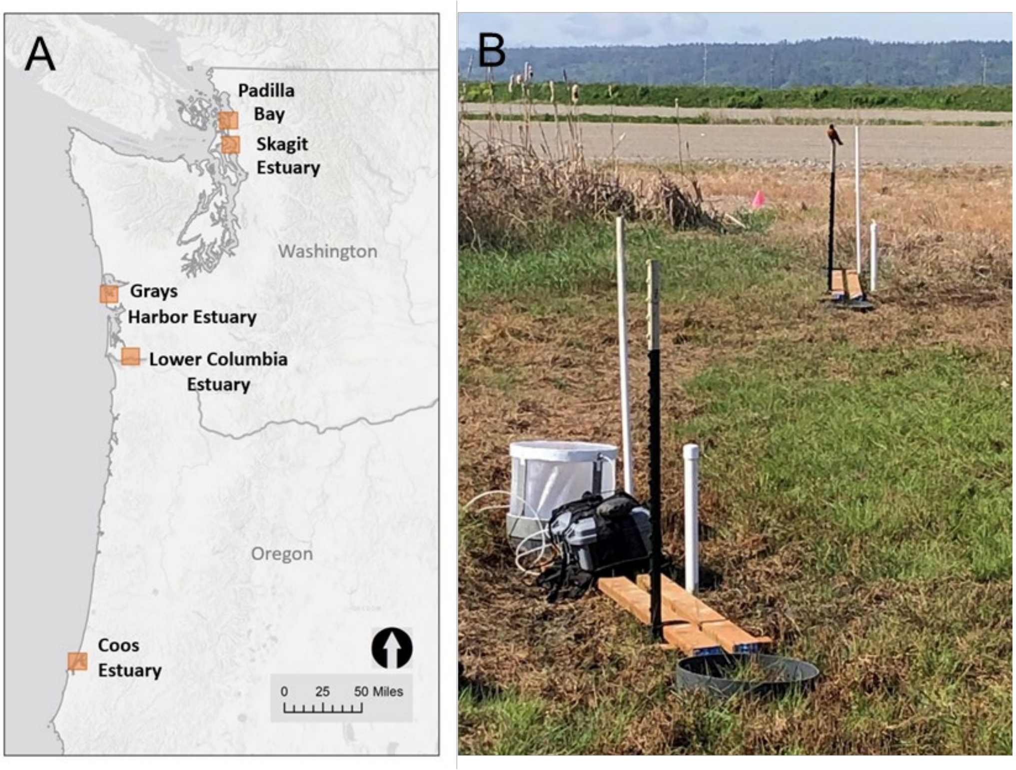

FIG. 1. (A) Map of the five study estuaries in Oregon and Washington, USA, and (B) example collar, boardwalk and chamber setup at a non-tidal pasture site in Padilla Bay. Photo by M. McKeon. Map by C. Cornu.

We determined the linear slopes of the change in GHG concentrations during light and dark periods to calculate flux rates. When linear slopes were non-significant ($R^2 < 0.33$ and $P > 0.05$), we concluded that fluxes were below the detection limit. Because the LI-COR instrument collected data at a much higher frequency than the Gasmet analyzer, almost all slopes from the former had a significant p-value, so the strength of the relationship (R^2) was the primary determinant of linearity with that instrument.

Environmental data

We installed one shallow groundwater well per pair of collars (3 per site) to obtain spot measurements of water-table level, water temperature, salinity, and pH at each gas sampling. These wells consisted of 1 m long, 3 cm diameter PVC pipes inserted halfway into the ground with drilled holes for the bottom 40 cm of the well to allow groundwater flow. At each GHG sampling event, we made measurements inside the wells with YSI Pro 30 conductivity meters (YSI Incorporated, Yellow Springs, OH) for salinity and Extech PH220 or Apera PH60 sensors for pH. Water-table measurements were individualized in the two chambers per boardwalk by measuring their respective elevations relative to the main groundwater well (see below).

We also established a single deeper (1.0-1.5 m) groundwater well at each site, typically located 15-20 m away from a major tidal creek or channel but relatively close to each transect, to obtain a detailed time series of groundwater conditions. These wells were constructed from 5 cm diameter PVC pipe and well screen. Inside each well we added a Hobo U20 or U20L (Onset Corporation, Bourne, MA) water-level sensor, suspended near the bottom of the well at a known distance below ground to record water-table level every 30 min. We also suspended an Odyssey conductivity and temperature logger (Dataflow Systems Ltd., Christchurch, NZ) about 25 cm below the ground surface to record salinity and temperature in the root zone every 30 min. In addition, we obtained a time series of soil temperature at each site by burying a Hobo pendant UA-001-08 logger 5 cm below ground and recording values every hour. During the >1 yr time series of soil temperature and groundwater conditions measured at each site, we periodically downloaded and cleaned loggers. We also checked for logger accuracy under controlled conditions before their use in the field, and verified logger salinity and temperature values with in situ checks performed with a YSI Pro30 conductivity probe. In a few freshwater sites we did not deploy Odyssey loggers in the groundwater wells, but did record salinity values with intermittent YSI Pro30 measurements.

Elevation

We determined the elevation of the wetland surface at each GHG collar and groundwater well using real-time kinematic global navigation satellite system (RTK-GNSS) methods with Trimble R8 and R12 rovers (Trimble, Inc., Westminster, CO) connected to real-time correction networks (ORGN in Oregon and southwest Washington and WSRN in the rest of Washington). For sites with significant tree cover, we determined elevations using laser leveling from nearby temporary benchmarks measured with RTK-GNSS. We obtained elevations in the North American Vertical Datum of 1988 (NAVD88) and converted values to an elevation scaled to local tidal datums using $z^* = (z\text{-MTL})/(\text{MHHW-MTL})$, where z is the measured NAVD88 elevation, and mean tide level (MTL) and mean higher high water (MHHW) are local tidal datums measured in NAVD88 (Swanson et al., 2014). For interpretation, $z^* = 0$ indicates a wetland at mean tide level, inundated about 50% of the time, and $z^* = 1.0$ is a wetland at local mean higher high water and is inundated much less frequently.

To compute z*, we obtained tidal datums (1985-2001 epoch) by processing time series of tidal channel water level collected near those sites with our own channel water level loggers, National Estuarine Research Reserve System water level stations (https://cdmo.baruch.sc.edu/), or NOAA tidal stations. We used VDATUM 3.6.1 and 4.1.2 for MTL estimates where needed. We processed water level time series using methodologies described in NOAA (2003).

Vegetation

For sites in the Coos and Columbia River estuaries, we obtained plant cover and height data during each GHG sampling event inside the chambers to quantify biomass and species composition. We visually determined percent cover of all species with at least 5% cover and measured height of up to four random shoots of each species. From these measurements we determined a "biomass index" by summing the product of average height and cover for all species.

Statistical analysis

For all statistical analyses we used R (v. 4.0.2 and 4.0.3, R Core Team 2020). We log-transformed CH_4 and N_2O data after adding a near zero minimal constant to all values to remove negative values. We compared light and dark fluxes of the two gases with paired t-tests. Because these indicated little difference, we averaged light and dark flux data for all subsequent analyses.

For the full dataset (all wetland types pooled), we tested for relationships between major environmental drivers and log-transformed CH_4 fluxes with linear regression. We used main well logger time series data as needed to fill in temperature and salinity data gaps in groundwater measures in the shallower wells at the time of gas sampling (for example when they were dry). Additionally, we explored whether environmental drivers sampled at each pair of chambers (such as salinity) were limiting factors (sensu Cade and Noon, 2003) on maximum CH_4 fluxes (estimated as the 0.95 quantile of the data distribution) with quantile linear regression using the R package "quantreg" (Koenker 2005).

A prior GHG flux study in two Oregon estuaries examined a number of different machine-learning techniques and determined that boosted regression trees (BRT) provided the best predictive power when multivariate environmental drivers are measured (Schulz et al., 2023). Therefore, we developed BRT models to analyze the interactive and non-linear effects of environmental drivers and wetland type on the full datasets of CH_4 and N_2O fluxes using the "gbm" package (Greenwell et al., 2022) and the "caret" package (Kuhn, 2021) for model training.

Boosted regression tree analysis is a machine learning method that sequentially combines multiple decision trees to develop a predictive model based on a matrix of continuous and/or categorical independent variables. This is done by training each subsequent tree by predicting the residual errors of the previous trees. The process of training multiple trees and combining their predictions is called "boosting." By boosting multiple decision trees in this way, BRT models can capture complex relationships and make accurate predictions even on noisy, nonlinear data. BRT models also assess the relative importance of independent variables in determining the total variance in the model. To visualize model outputs we used Individual Conditional Expectation (ICE) curves, which are an expansion of Partial Dependence Plots (PDPs). While PDPs show the average marginal effect on the response variable, ICE curves depict the change in the predicted response variable for each observation as each predictor variable varies. The centered ICE makes clearer any pronounced heterogeneity in our results.

After developing the BRT model for CH_4 based upon the point measures of fluxes and their paired environmental data, we implemented a slightly simplified version of the explanatory model in the predictive mode to estimate annual gas fluxes at the site level (n=34). The environmental data we used to estimate annual fluxes were the one-year time series data collected at each site at 30 minute intervals including water-table level, groundwater salinity, groundwater temperature from continuous logging in the main wells, soil temperature from continuous logging at the main well, air temperature from near-by weather stations, and one-time points measurements of site elevation at the larger groundwater well, and the five categories of wetland class. We reran BRT models without groundwater pH in annual predictions since we did not have continuous site pH data over the study period (parameters only changed slightly). Predicted CH_4 fluxes per 30 min intervals were summed over one year to give an annual total per site. We chose not to estimate annual N_2O fluxes because of the relatively poor predictive power of the BRT model and their very low values (see below).

To test for differences across the five wetland types examined in this study (reference marsh, reference swamp, restored marsh, wet pastures, and dry pastures), we used parametric Welch's one-way ANOVA and Games-Howell post hoc tests. We also reran this test after subdividing the flux measurements into wet (October-May) and dry (June-September) seasons.

For sites in the Coos and Columbia River estuaries, we examined relationships between GHG fluxes and plant metrics. We tested for relationships between GHG fluxes and the biomass index using linear regression. To examine potential linkages between plant community structure and GHG fluxes, we subset plant cover data inside the GHG chambers collected in the summer season (June-Aug 2021) and applied 2-dimensional non-metric multidimensional scaling (NMDS) to separate chambers by species composition using the R package "vegan" (v.2.6-2; Oksanen et al., 2022) and a Bray-Curtis dissimilarity matrix based on Wisconsin double-transformed cover data (Oksanen, 2015). A convergent solution was obtained after 20 iterations performed with function "MetaMDS" and step-across similarities because many chambers had little overlap in species composition. On the NMDS plots, we overlaid centroids of selected plant species as well as contours of CH_4 and N_2O fluxes using function "ordisurf" in "vegan," which relates the dependent variable (GHG flux) to species composition in the ordination space with a general additive model.

RESULTS

Environmental drivers of CH_4 fluxes

There was no significant difference in CH_4 fluxes between light and dark conditions (t = -0.03, df = 1338, P = 0.98). Fluxes ranged from negative (uptake or consumption) to positive (emissions) values, with 16% of values showing CH_4 uptake or consumption, 16% showing non-detectable fluxes (treated as zeros), and 68% of values showing emissions to the atmosphere.

Linear relationships between CH_4 fluxes and key environmental drivers were weak due to substantial variability (low R^2) although often statistically significant (low P-values) within the large dataset (Table 1). Groundwater salinity, pH, and wetland elevation had negative relationships with CH_4 flux, while water-table level and groundwater temperature had positive relationships with CH_4 flux (Table 1; Appendix S1: Fig. S1). The upper bounds of the CH_4 distribution with individual environmental drivers (e.g., an estimate of maximum short-term fluxes) similarly were positively or negatively related to these drivers indicating that several abiotic factors may have roles as limiting factors for CH_4.

TABLE 1. Summary of linear relationships between point measurements of CH_4 fluxes and individual environmental drivers in PNW tidal wetlands shown in Appendix S1: Fig. S1.

Environmental driver	**Model fits to fluxes**			**Model fits to maximum fluxes**	
	Slope	**R^2**	**P**	**Slope**	**P**
Salinity	-0.007	0.018	<0.001	-0.039	<0.001
Water-table level	0.277	0.060	<0.001	1.206	<0.001
Wetland elevation	-0.120	0.020	<0.001	-1.160	<0.001
Groundwater pH	-0.103	0.018	<0.001	-0.628	<0.001
Groundwater temp	0.011	0.006	<0.01	0.052	0.13
Soil temperature	0.008	0.001	0.12	0.036	0.04
Air temperature	-0.002	-0.0002	0.42	-0.006	0.62

Notes: We fit fluxes with least-squares regression as well as maximum fluxes (0.95 quantile of the distribution) using quantile regression.

We tuned the CH_4 BRT model using 2,432 trees with an interaction depth of 16 and a learning rate of 0.01, and 11 as the minimum number of observations per node. The adjusted R^2 between the model trained with the full data set against the full data set was 0.86, indicating that it effectively captured the multi-factor, nonlinear controls over CH_4 fluxes. Three environmental drivers had a relatively strong influence on CH_4 fluxes in the BRT model, with wetland elevation accounting for 21.0% of relative influence, followed by salinity (18.3%), and water-table level (16.0%) (Fig. 2; Appendix S1: Table S2). Wetland type, pH, and air, soil and groundwater temperature all had smaller relative effects on CH_4 fluxes in the model (each < 15%).

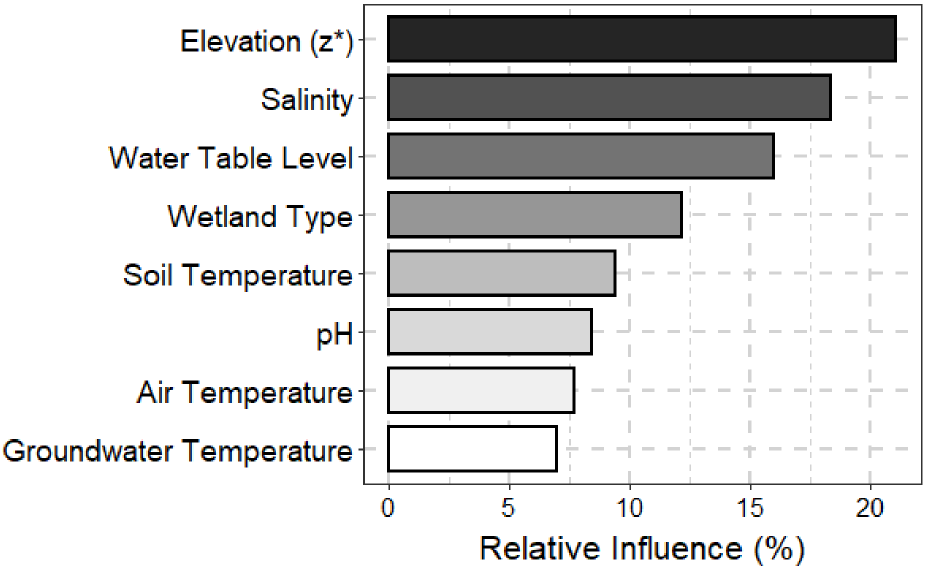

FIG. 2. The relative influence of eight environmental variables on point measurements of CH_4 fluxes in the BRT model for PNW coastal wetlands. The adjusted R^2 between modeled and measured fluxes was 0.86.

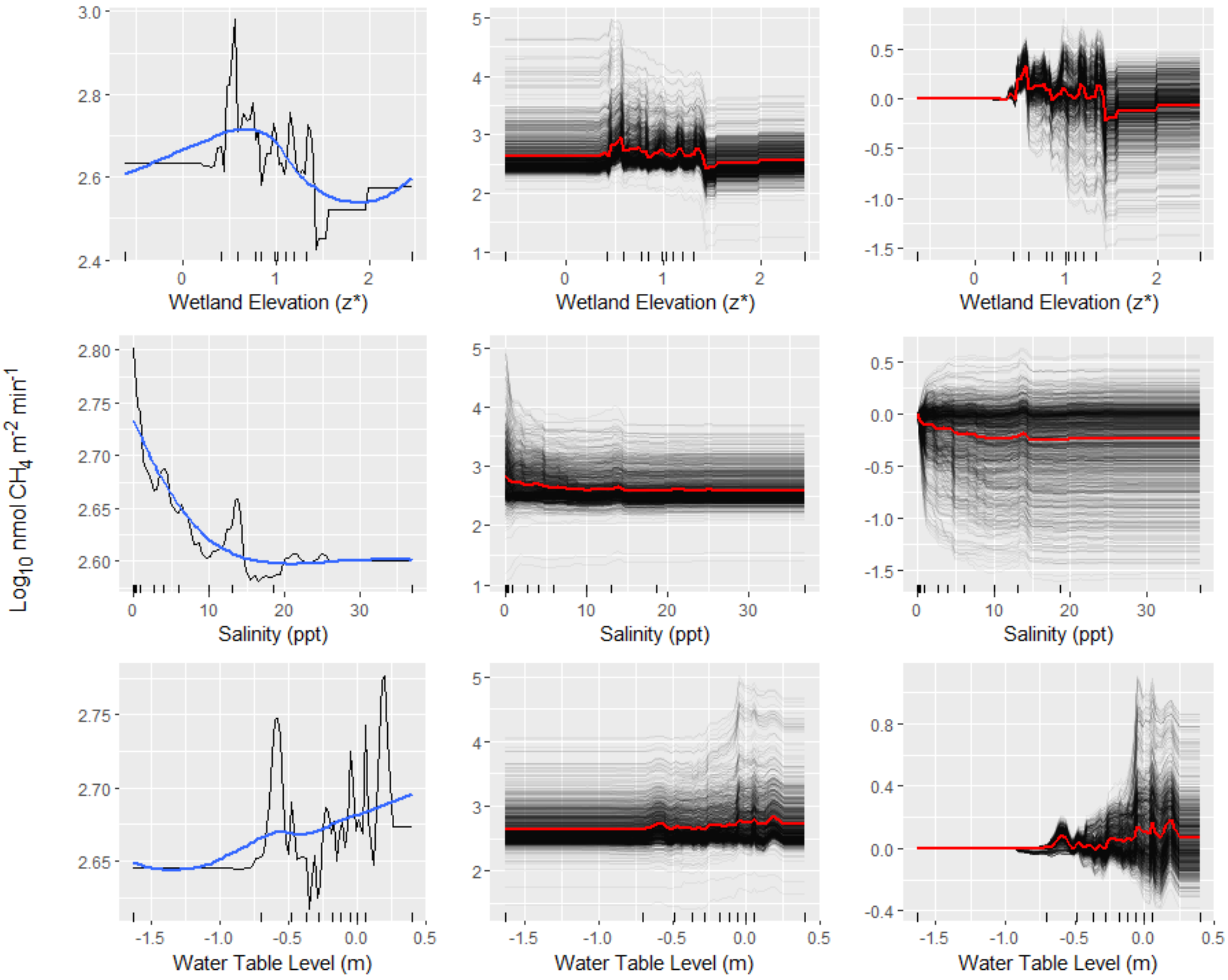

FIG. 3. Partial (left), ICE (center) and ICE-centered (right) plots of point measurements of CH_4 fluxes and the three most influential variables in the BRT model. Loess-smoothed lines are in blue (left) or red (center, right). Rugs on the x-axis denote 10% quantiles of data. Partial plots show the influence of single variables on fluxes with other variables held constant.

Wetland elevation, water-table level, and salinity—the three most important variables in the BRT model—had non-linear relationships with CH_4 fluxes when other variables were held constant (Fig. 3). The highest positive flux values were observed at wetland elevations between about z* = 0.5 and z* = 0.8 (elevations somewhat below local MHHW). Furthermore, there was a dramatic decrease in CH_4 flux at about z* = 1.4, corresponding to sites that were very infrequently inundated or not at all. Methane fluxes increased with higher water-table levels up to and above the surface (e.g., surface ponding), while deeper water-table levels (> 0.5 m below the surface) were associated with lower CH_4 fluxes. Methane fluxes declined non-linearly but monotonically with salinity, and when other variables were held constant, the lowest fluxes occurred at groundwater salinities above 15 ppt.

CH_4 fluxes and plant biomass and composition

Total plant biomass inside the chambers, estimated as percent cover times height, was positively but only weakly linearly correlated with CH_4 fluxes ($r^2 = 0.08$, $P < 0.001$; Fig. 4). In the NMDS plot of species composition with general additive models to visualize change in summer-time CH_4 fluxes across the two-dimensional ordination, the highest CH_4 fluxes were observed in plots that tended to have a greater relative abundance of fresher species such as *Phalaris arundinacea* (reed canarygrass; a regionally invasive grass) and *Sagittaria latifolia* (wapato; a native forb) (Fig. 5). In contrast, chambers dominated by regionally common native halophytic species such as *Salicornia pacifica* (pickleweed), *Distichlis spicata* (salt grass), and *Jaumea carnosa* (fleshy jaumea) had little to no CH_4 emissions or CH_4 uptake.

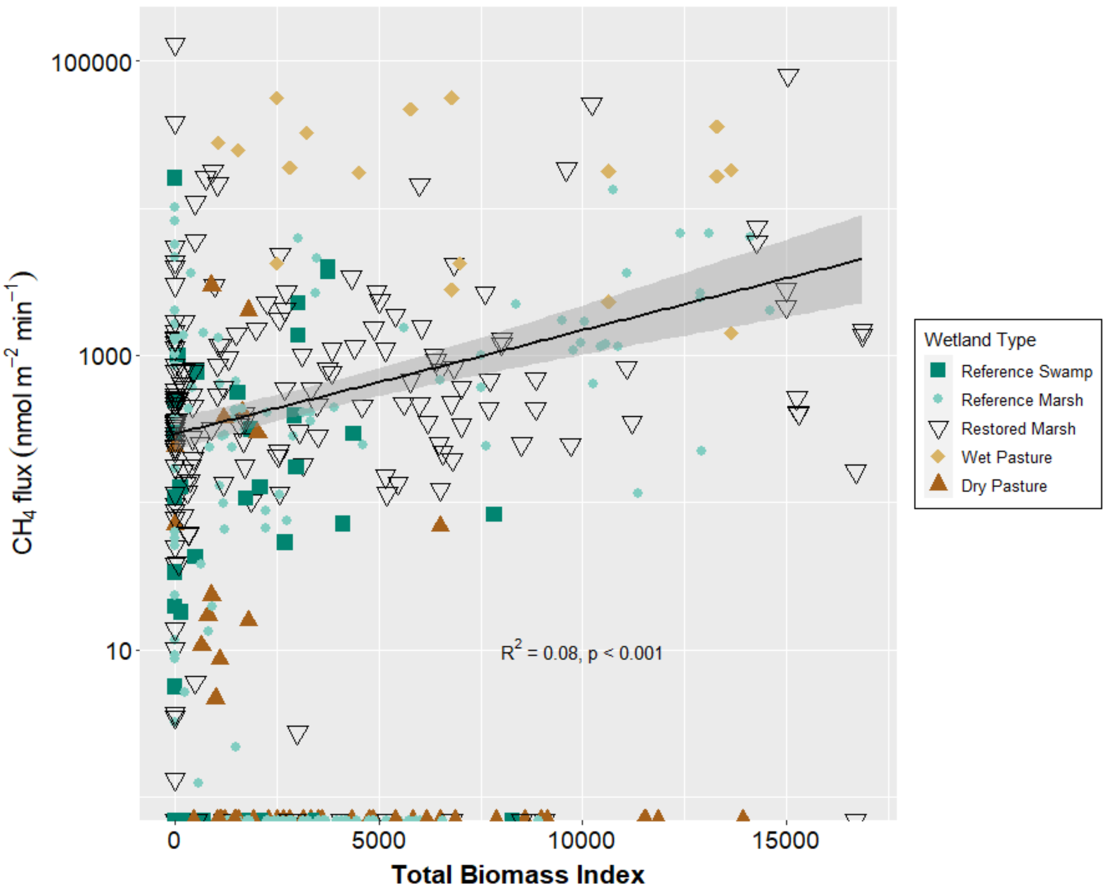

FIG. 4. Relationship between plant biomass index and point measurements of CH_4 fluxes ($\log_{10}$ scale). Data are from only the Coos and Columbia River estuaries, but include all sampling dates over the course of a year.

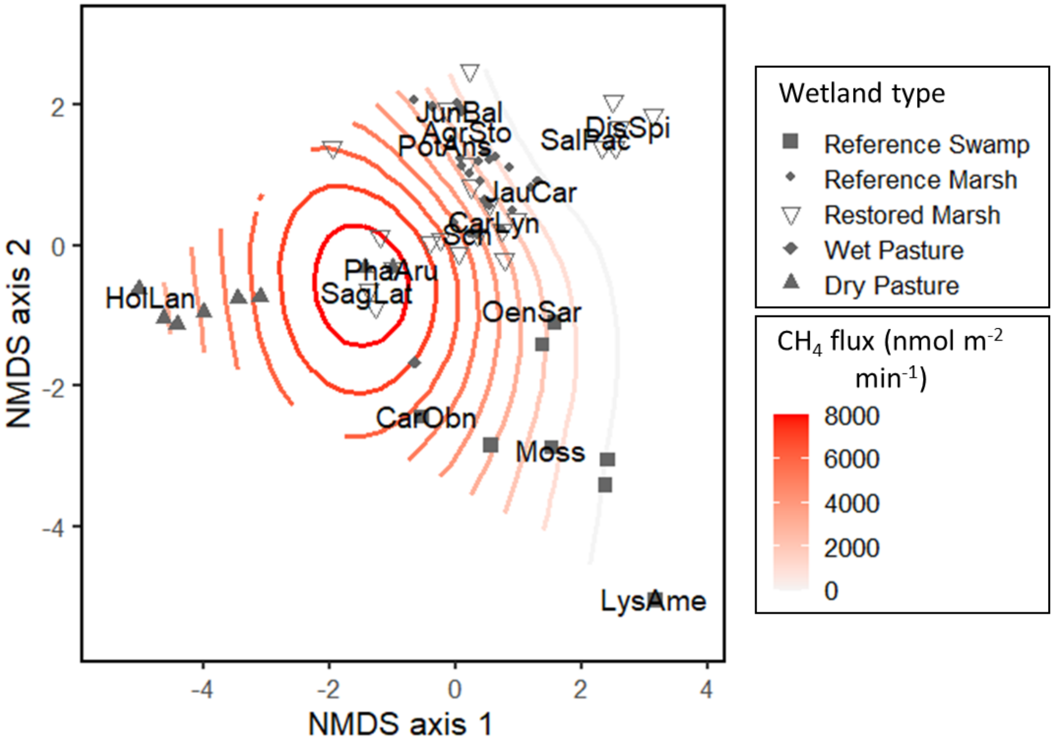

FIG. 5. Relationship between plant species composition in two dimensional NMDS space and point measurements of CH_4 fluxes during summer sampling in the Coos and Columbia River estuaries. Individual chambers are indicated by points. The centroids of common and indicator species are given by three-letter codes as in Appendix S1: Table S3. Modeled CH_4 fluxes across the species compositional space are indicated by color contours.

Wetland type effects on environmental drivers and point-measurements of CH_4 fluxes

Large differences in environmental drivers among wetland types (Fig. 6) largely subsumed the effect of type in the CH_4 BRT model (wetland type relative influence = 12.1%, Fig. 2). Reference marshes had the highest groundwater salinity followed by restored marshes and then other wetland classes. Restored marshes had the highest water-table levels, followed by reference marshes and wet pastures. Wetland elevations were significantly higher in tidal swamps than in reference marshes, restored marshes, and wet pastures (while dry pastures were highly variable since they included three subsided former tidal wetlands and two pastures above tidal influence). Air, soil, and water temperature largely reflect seasonality, so differences among sites were small, with tidal swamps being slightly cooler, and wet pastures slightly warmer (results not shown). Groundwater pH average and median across wetland type remained relatively consistent between 6.2 and 6.4.

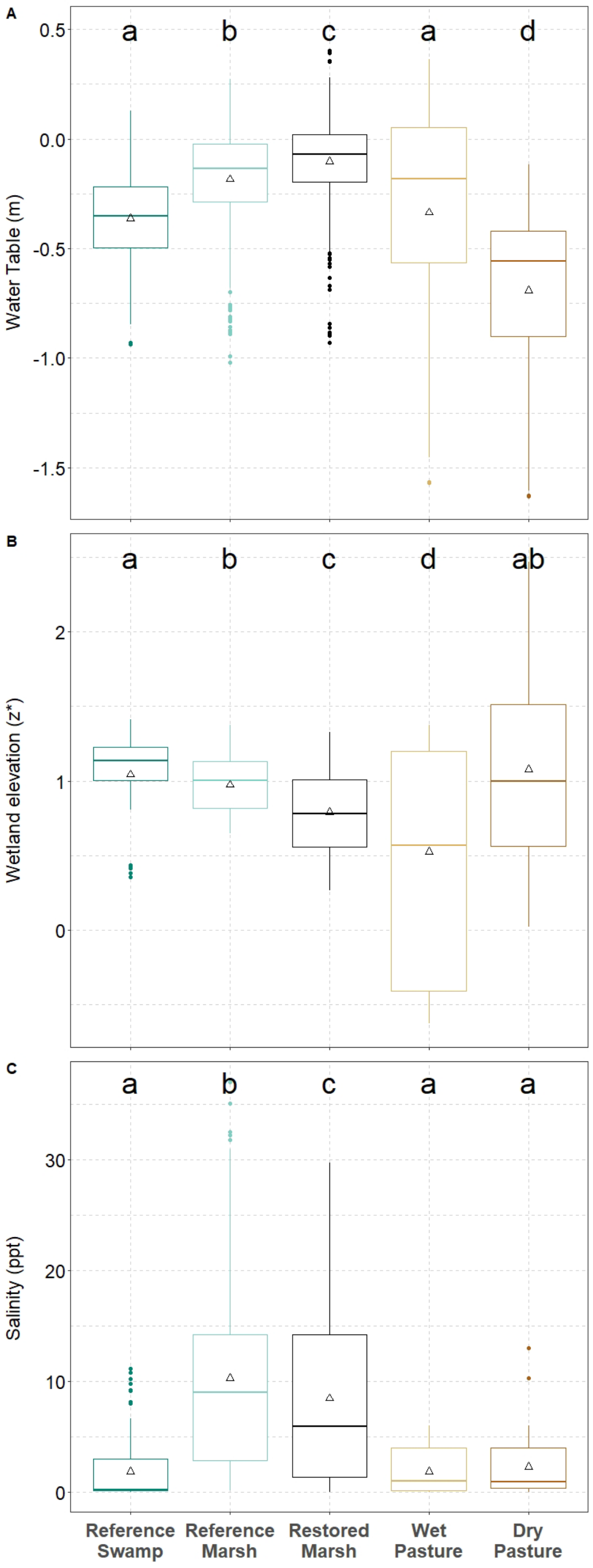
A
a
b
c
a
d
0.5
0.0
-0.5
-1.0
-1.5
Water Table (m)
B
a
b
c
d
ab
2
1
0
Wetland elevation (z*)
C
a
b
c
a
a
30
20
10
0
Salinity (ppt)
Reference Swamp
Reference Marsh
Restored Marsh
Wet Pasture
Dry Pasture

FIG. 6**.** Boxplots of differences in water table (A), elevation (B), and groundwater salinity (C) by wetland type. Median = solid lines, mean = triangles. Unshared letters denote significant differences (Welch's ANOVA, Games-Howell Tests).

When examined in isolation, CH_4 fluxes integrated over the duration of the study varied substantially among wetland types ($n = 1412$, $W = 47.4$, $df = 4$, $P < 0.001$; Fig. 7A; Appendix S1: Table S4). The highest fluxes occurred in restored marshes and wet pastures. There was considerable variation in values within wetland classes; for example, in wet pasture sites, fluxes ranged from -31 to ~200,000 nmol m^{-2} min^{-1}. Average fluxes were slightly higher in the dry season (which is also warmer), except in pasture sites. Wet pasture sites had the highest CH_4 emissions in the study, whereas dry pasture sites had the highest uptake value recorded (Appendix S1: Table S4). Restored marshes had maximum fluxes over 10 times higher than those in both reference tidal swamps and marshes.

During the wet season (October - May), CH_4 fluxes were significantly higher in restored marshes and wet pastures than in reference marshes and swamps, and significantly lower in dry pastures ($n = 983$, $W = 28.4$, $df = 4$, $P < 0.001$; Fig. 7B). This pattern was similar for dry season conditions (June - September) except that wet pasture fluxes were highly variable and not different from any of the tidal wetland classes ($n = 429$, $W = 47.8$, $df = 4$, $P < 0.001$; Fig. 7C).

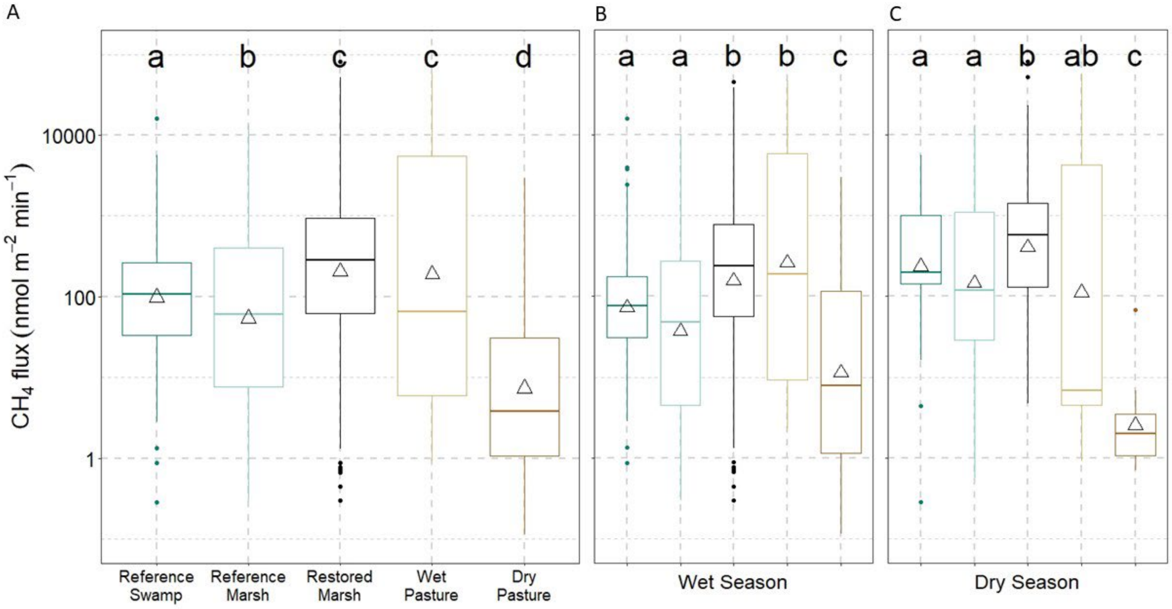

FIG. 7. Boxplots of point measurements of CH_4 flux by wetland type in all seasons (A) and separated into wet (B) and dry (C) seasons in PNW estuaries ($\log_{10}$ scale). Median = solid lines in the box plots, mean = triangles. Wetland classes not sharing the same lowercase letters were significantly different.

Estimated annual CH_4 fluxes

Using the output from the BRT model and time series data, we estimated annual CH_4 fluxes over 2021-2022 (Table 2). To increase representation within our geographic study area, we included annual CH_4 fluxes from three additional reference sites and six additional restored sites in a large recently restored emergent marsh in Tillamook Bay, Oregon reported by an earlier study that used a similar BRT modeling approach (Schulz et al., 2023). Annual fluxes are similar to those for point measurements, showing the highest annual CH_4 fluxes in restored marshes and wet pastures.

TABLE 2. Annual CH_4 fluxes for wetland classes predicted from the BRT model. Included are all sites from this study, and three additional reference marshes and six additional restored marshes in Tillamook Bay, OR reported by Schulz et al. (2023).

Predicted CH_4 flux (g CH_4 m^{-2} yr^{-1})						
Wetland Class	**N**	**Mean**	**SE**	**Median**	**Max**	**Min**
Reference Swamp	5	0.56 a	0.15	0.58	0.96	0.08
Reference Marsh	15	4.44 b	2.18	2.03	34.61	0.75
Restored Marsh	15	36.30 b	27.77	3.94	420.03	0.46
Wet Pasture	3	37.25 ab	34.61	3.60	106.46	1.70
Dry Pasture	5	0.21 ab	0.84	0.14	3.26	-1.39

Notes: Unshared letters in the mean column denote significant differences (Welch's ANOVA, Games Howell tests).

We also examined annual fluxes relative to average annual salinity and wetland elevation. Similar to the point measurements (Appendix S1: Fig. S1), there was wide variability in annual CH_4 fluxes at salinities < 3 ppt, but a much narrower range of fluxes at higher salinities (Fig. 8A). The result of this variability was that salinity classes were not significantly different whether fresh and oligohaline classes were separated or combined (Welch's ANOVA $p > 0.60$, Table 3). Annual and point measurements of fluxes by wetland and salinity classes are given in Appendix S1: Tables S4 and S5. Higher annual CH_4 fluxes (> 10 g CH_4 m^{-2} yr^{-1}) were only observed in lower elevation wetlands, where $z^* < 0.75$ (Fig. 8B).

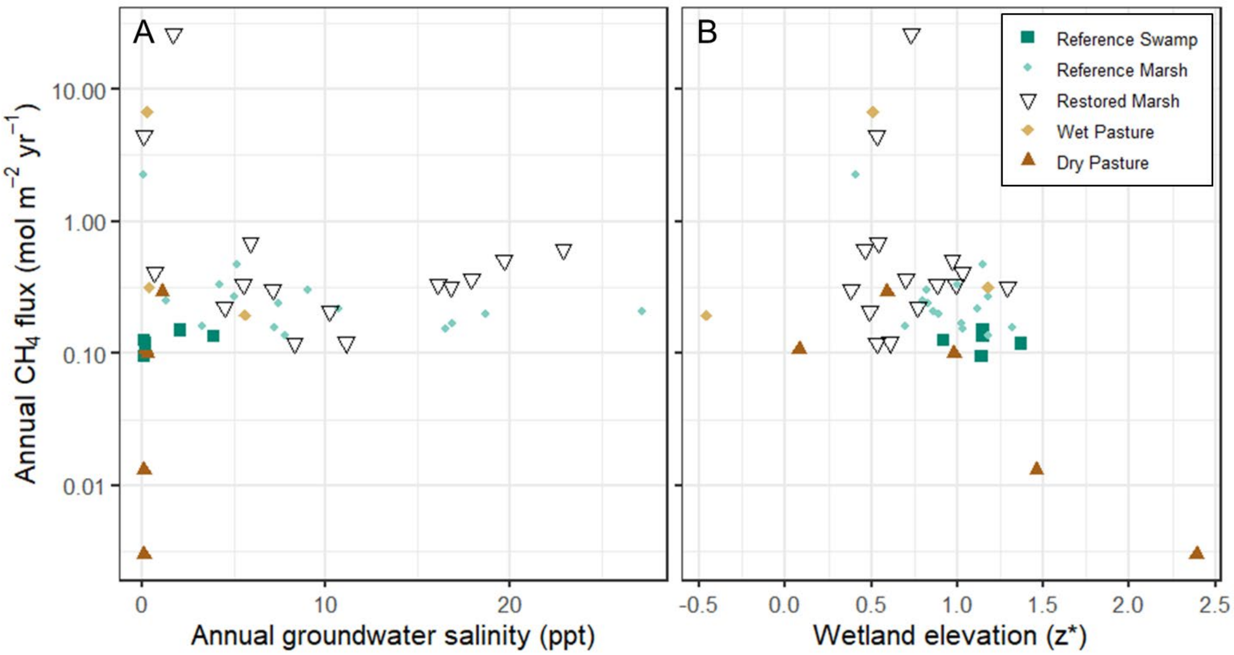

FIG. 8. Log_{10} annual CH_4 flux (plus a constant of 1.393) relative to (A) average annual groundwater salinity and (B) standardized tidal elevation (z*) from 34 sites in this study and nine sites in Schulz et al. (2023). Wetland classes are shown by different colors and shapes. The insets show non-logged results without the added constant.

TABLE 3. Annual CH_4 fluxes for salinity classes predicted from the BRT model. Included are all sites from this study and two oligohaline and seven mesohaline sites in Oregon from Schulz et al. (2023).

Predicted CH_4 flux (g CH_4 m^{-2} yr^{-1})						
Salinity Class	**N**	**Mean**	**SE**	**Median**	**Max**	**Min**
Fresh	11	19.45	11.01	0.46	106.46	-1.39
Oligohaline	10	44.27	41.75	2.73	420.03	0.72
Mesohaline	18	2.86	0.54	2.20	9.61	0.46
Polyhaline	4	4.67	1.69	4.28	8.36	1.74

Environmental drivers of nitrous oxide fluxes

As with CH_4 fluxes, there was no significant difference in N_2O fluxes under dark versus light conditions (t = 1.31, df = 445, P = 0.19), and therefore we averaged light and dark fluxes for each chamber measurement. The majority of flux measurements (89.5%) were below the detection limit (treated as zeros), while 8.4% were emissions and 2.1% were uptake.

Nitrous oxide fluxes were only significantly linearly related to water-table level but with low predictive power ($R^2 = 0.030$, Appendix S1: Table S6). In the BRT model, the environmental drivers explained a modest amount of the variation in measured fluxes (adjusted $R^2 = 0.25$). Wetland type was the strongest predictor of N_2O fluxes (22.0%) while other factors had lower relative importance, including water-table level (19.3%), wetland elevation (15.9%), and salinity (12.2%) (Fig. 9; Appendix S1: Table S2).

Total plant biomass was not significantly correlated with N_2O fluxes ($R^2 = 0.007$, p = 0.32). When chambers were evaluated in terms of species composition, the highest N_2O fluxes tended to be associated with *Holcus lanatus* (a non-native grass found in dry pastures) while the lowest fluxes were associated with native freshwater wetland species such as *Carex obnupta*, *Oenanthe sarmentosa*, and mosses (Appendix S1: Fig. S2).

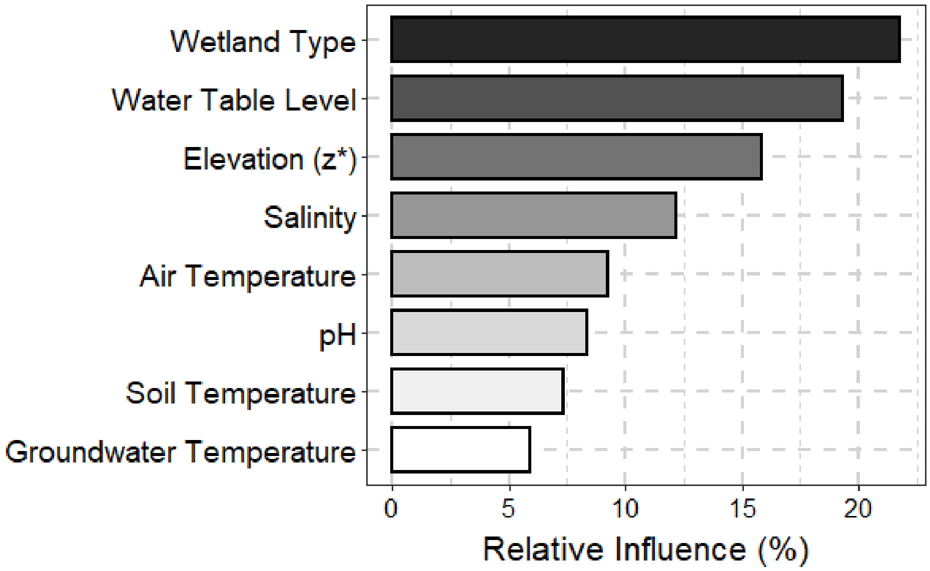

FIG. 9. The relative influence of eight environmental variables on point measurements of N_2O fluxes in the BRT model for PNW coastal wetlands. The adjusted R^2 between the model and measured fluxes was 0.25.

Wetland type effects on nitrous oxide fluxes

Nitrous oxide fluxes differed significantly by wetland class (chi-squared = 32.876, df = 4, $P < 0.001$), although their medians were all zero (Appendix S1: Table S7). Dry pasture sites had higher fluxes than wet pastures, reference and restored marshes, and tidal swamps (post-hoc Dunn’s test). Least-disturbed marshes showed the greatest variability in fluxes with a maximum of 49 and a minimum of -60 nmol N_2O m^{-2} min^{-1}. Reference and restored marshes each showed approximately equal flux ranges above and below zero.

DISCUSSION

Blue carbon ecosystems are recognized as potential contributors to natural climate solution initiatives to help mitigate anthropogenic emissions. Because GHG emissions, particularly CH_4, may partially or completely offset the substantial carbon sequestration rates of tidal wetlands (Bridgham et al. 2006, Al-Haj and Fulweiler 2020, Rosentrenter et al. 2023), and could thus limit the viability of estuarine wetlands as a climate mitigation strategy (Silva et al., 2022; Johannessen and Christian 2023), it is essential to quantify their effects on the potential climate benefits of conserving and restoring tidal wetlands. It also is important to predict the local and regional variability of GHG fluxes associated with those activities for the benefit of planners, land managers, policy makers, and others developing natural climate solution initiatives and prioritizing actions.

To address these issues, we collected a large dataset of CH_4 and N_2O fluxes and associated environmental drivers across multiple wetland types and management regimes in estuarine wetlands in the PNW and compiled these new data with previously reported regional data for analysis. Our results identify the degree of soil saturation (as indicated by both water-table level and wetland surface elevation) and groundwater salinity as major drivers of CH_4 fluxes. In turn, the effects of wetland type and management on GHG fluxes was largely mediated through their effects on these environmental drivers.

Reflecting the current and legacy effects of land management on these environmental drivers, wet pastures and restored marshes (mostly previously diked pastures) had the highest CH_4 fluxes, albeit with high variation among sites. In a more limited dataset from sites in only two estuaries, N_2O fluxes were uniformly low across all wetland types and land management regimes with a median of zero, suggesting this is not an important GHG in many PNW estuarine wetlands. We show that a machine learning approach can be used to estimate annual CH_4 fluxes across heterogeneous landscapes if key environmental time series data are collected, and the regional models developed should allow extrapolation to other tidal wetland sites in the PNW.

Environmental controls of CH_4 fluxes

Our results largely support our first hypothesis that CH_4 fluxes increase with higher water tables, lower salinity, and higher soil and air temperatures. Additionally, the machine learning model supported our second hypothesis that these variables had non-linear and interactive effects. The environmental drivers individually had poor, even if often statistically significant, linear relationships with CH_4 fluxes (Table 1, Appendix S1: Fig. S1). However, BRT modeling successfully captured these complex relationships, explaining 86% of the variation in CH_4 fluxes, which improves upon previous BRT modeling of CH_4 fluxes in two Oregon estuaries using a somewhat different set of environmental driver variables ($R^2 = 0.77$, Schulz et al., 2023). The most important variables in the BRT model were related to hydrology, with wetland elevation relative to tide range (a proxy for surface inundation at tidal sites) and water-table level (important at both tidal and non-tidal sites) together explaining 37% of the variance (Fig. 2). Salinity was also important, explaining 18% of the variance. The partial plots from the BRT model demonstrated the nonlinear relationship of these variables with CH_4 fluxes (Fig. 3).

We expected variables relating to the degree of waterlogging to be important in explaining CH_4 fluxes because methanogenesis is an obligatory anaerobic process and aerobic CH_4 oxidation requires oxygen (Megonigal et al., 2004). Our results emphasize the importance of measuring site elevation normalized to tide range (z*) as a predictive variable for CH_4 fluxes in tidal wetlands, similar to the findings of Arias-Ortiz et al. (2024) in a synthesis of CH_4 fluxes across tidal wetlands in the conterminous U.S. In comparison, water-table level can be more problematic as a predictive variable for point chamber measurements of gas fluxes because these measurements are often taken during low tides and in daylight hours. We sampled all but the lowest elevation tidal sites randomly through the daylight hours, which should reduce the tidal bias in our analysis (potential daylight sampling biases are discussed below). The effect of water-table level can also be complicated. For example, a PNW salt marsh chamber study with continuous diel sampling found that CH_4 flux decreased during a storm surge, which was ascribed to hydrostatic pressure inhibiting diffusion and ebullition (i.e., bubble release) (Diefenderfer et al., 2018a). Similarly, eddy covariance studies often find pulses of CH_4 flux around low tides, suggesting that the inhibiting effect of hydrostatic pressure may be a wide-spread phenomenon (Ariaz-Ortiz et al., 2024).

Salinity was the second most important variable in our CH_4 BRT model (Fig. 2). It is recognized as an important predictor of CH_4 fluxes in tidal wetlands because it is a surrogate for less easily measured sulfate concentrations (Poffenberger et al., 2011). Seawater has relatively high concentrations of sulfate, and sulfate-reducing bacteria in wetlands are competitively superior to methanogens for substrates (Megonigal et al., 2004). However, variability in this relationship can be high because of the local depletion of groundwater sulfate under saline conditions (Poffenberger et al., 2011). We found very high modeled annual fluxes of CH_4 (i.e., > 10 g CH_4 m^{-2} yr^{-1}) only at salinities less than about 2 ppt, albeit with substantial variation due to interacting factors such as water-table level and site elevation (Fig. 8). Both measured data (Appendix S1: Fig. S1) and the BRT model (Fig. 3) of instantaneous fluxes showed a slight spike in CH_4 emissions at about 15 ppt salinity, but this result was not evident in the annual estimates.

Thus, we conclude that some, but far from all, fresh and oligohaline tidal wetlands in the PNW emit large amounts of CH_4. Similar results have been found in syntheses over broader geographic areas (Poffenbarger et al., 2011; Windham-Myers et al., 2018; Al-Haj and Fulweiler, 2020, Arias-Ortiz et al., 2024). We return to the management implications of these findings below.

The relatively low influence of temperature in our CH_4 BRT model (Fig. 2) was surprising given the strong theoretical foundation for temperature effects on methanogenesis (Wu et al., 2021) that typically is translated into robust empirical relationships across wetland sites. For example, temperature was a dominant predictor of CH_4 fluxes in both chamber studies and eddy covariance studies in tidal wetlands across the conterminous U.S. (Arias-Ortiz et al., 2024). Apparently, in our dataset, the gradients of salinity and waterlogging among sites were more important than the relatively muted seasonal temperature changes along the PNW coast in controlling CH_4 fluxes. However, in our previous study of CH_4 fluxes in two Oregon estuaries, temperature was the most important predictor of CH_4 fluxes in the BRT model (Schulz et al., 2023).

Plant controls of GHG fluxes

Our third hypothesis was that plant biomass and community composition would affect GHG fluxes. There was a weak, but significant, relationship between our plant biomass index on CH_4 fluxes (Fig. 4), but not on N_2O fluxes. Plant community composition was also related to both CH_4 and N_2O fluxes (Fig. 5, Appendix S1: Fig. S2). The highest CH_4 fluxes tended to be associated with plots with greater abundance of *Phalaris arundinacea* and *Sagittaria latifolia*, most likely reflecting the preference of these species for freshwater conditions (Borde et al., 2020). *P. arundinacea* is a regionally common invasive grass which often dominates diked former tidal wetlands but also occurs in fresher tidal sites. *S. latifolia* is a native forb common in tidal freshwater wetlands in the Columbia River Estuary. Plants also can have direct effects on wetland CH_4 fluxes by affecting CH_4 transport from the soil to the atmosphere, diffusion of O_2 into the root zone, and by providing labile substrate (Laanbroek, 2010; Bridgham et al., 2013; Vroom et al., 2022). However, differences in species composition and their physiological traits may not drive GHG fluxes per se, since differences in plant composition in tidal wetlands often closely reflect the same major environmental drivers that affect CH_4 fluxes such as inundation (elevation) and salinity (Watson and Byrne, 2009; Janousek and Folger, 2014). Other studies have similarly found that plant species composition can be an effective predictor of CH_4 fluxes because of these indirect relationships between plant environmental tolerances and environmental drivers of CH_4 flux (Bubier et al., 1995; Dias et al., 2010). Plants likely have the same range of effects on N_2O fluxes, but plant effects are complicated by the multiple pathways of N_2O production and consumption discussed below. Also, the low N_2O fluxes measured in this study would tend to reduce any strong associations with plant biomass or composition.

We found no effect of light versus dark conditions on the fluxes of either CH_4 or N_2O, but this is not the equivalent of finding that there were no day versus night differences. For example, a previous study found that a PNW salt marsh had greater nighttime than daytime CH_4 fluxes (Diefenderfer et al., 2018a). We may have observed limited light versus dark differences in GHG fluxes because plant stomata typically close upon intermittent darkness after a lag period of tens of minutes (Lawson and Blatt, 2014), so our short incubation conditions may have had limited effects on plant gas transport. Furthermore, the wetland plants in our plots were primarily herbaceous emergent species that occur in shallower water, where passive diffusion is the dominant mode of gas flow (Vroom et al., 2022). Diffusive gas flow through plants is limited mainly by root properties, and accordingly, there is typically no diel pattern in gas flux from these plants (Vroom et al., 2022). To our knowledge, only one taxon in our dataset, *Schoenoplectus* spp., has limited capability for pressurized gas flow where stomatal effects on gas fluxes would be expected to be more important (Vroom et al., 2022). Finally, there were also limited chamber effects on air or soil temperatures with our short incubation times, so typical diel temperature changes were not represented by our light versus dark incubation conditions.

Wetland type and management effects on CH_4 fluxes

We confirmed our fourth hypothesis that CH_4 fluxes differ among estuarine wetland types and land management regimes, which can largely be explained by their effects on the ecosystem drivers of fluxes such as elevation and water-table level. Furthermore, our study indicated that the highest CH_4 fluxes occurred in sites that are fresher and more waterlogged, such as non-tidal wet pastures and lower salinity restored sites (Fig. 8). Wetland type (which included management categories) was only the fourth most important factor in the CH_4 BRT model, explaining 12.1% of the variation (Fig. 2). This relatively lower importance may be due to our finding that the important environmental drivers of CH_4 flux (elevation, salinity, and water-table level) also differed substantially among wetland types (Fig. 6). Thus, wetland type and management have a large effect on the environmental factors that ultimately control CH_4 fluxes. A similar conclusion emerged from our previous study using BRT modeling in the PNW (Schultz et al., 2023). Temperature variables were less important in the BRT model in the current study but would be expected to reflect diel and seasonal effects rather than site effects in a regional analysis with limited variability in climate regime (Appendix S1: Table S1).

Consistent with Schultz et al. (2023), we found that restored marshes and wet non-tidal pastures tended to have the highest average, median, and maximum CH_4 fluxes, but there was wide variation within these wetland categories (Tables 2 and 3). Both restored marshes and wet pastures tended to be at lower elevations than reference sites, reflecting prior subsidence from drainage and soil compaction (Fig. 6). Restored marshes had high water-table levels and variable salinity, whereas wet pastures had variable water-table levels and low salinity. Accordingly, two of three low salinity restored marshes had very high annual CH_4 fluxes (Fig. 8). Wet pastures were distinctly more waterlogged than dry pastures but they still had substantial variation in water tables (Fig. 6), which led to their large variation in CH_4 fluxes.

N_2O fluxes

We also confirmed our fifth hypothesis that N_2O fluxes are low overall, but are somewhat higher in non-tidal pastures. The median N_2O flux was zero in all wetland types, but average and maximum fluxes were somewhat higher in dry pasture sites (Appendix S1: Table S7). All wetland types also had a substantial number of significantly negative N_2O fluxes. Our findings agree with other studies in the PNW and elsewhere that wetlands have low N_2O fluxes unless they have substantial external nitrogen inputs (Mosemann-Valtierra, 2012; Diefenderfer et al., 2018a; Schultz et al., 2023).

Because the majority of our N_2O measurements were below detection level, the BRT model did a relatively poor job of predicting drivers of fluxes ($R^2 = 0.25$). This result is perhaps not surprising given that N_2O is produced by several processes within the nitrogen cycle, which have very different environmental controls, and different components of the denitrification process produce and consume N_2O (Baggs, 2011; Butterbach-Bahl et al., 2013). Reflecting the inability of the BRT model to capture important environmental drivers of N_2O fluxes, wetland type was the most important variable in the model (Fig. 9).

These results are substantially similar to our previous study of GHG fluxes in two Oregon estuaries, where N_2O fluxes had a median of zero and the BRT model only predicted 11% of the total variance (Schultz et al., 2023). In that study we found that former tidal wetlands in agricultural use and restored sites had the highest (but still low) N_2O fluxes, suggesting that sites restored from an agricultural legacy may retain some legacy effects that promote slightly higher N_2O fluxes.

Synthesis and management considerations

This study demonstrates that machine-learning techniques, combined with an appropriate set of environmental driver data, are a powerful tool for estimating GHG fluxes from tidal wetlands. This approach may provide an alternative to intensive chamber-based or flux tower measurements, which are labor intensive and expensive and, therefore may not be feasible for many tidal wetlands where assessment of GHG fluxes is needed to understand the radiative forcing of these ecosystems. Our results can be directly used in other tidal wetlands in the PNW. A similar approach in other regions would require collecting GHG flux and environmental driver data across the spectrum of wetland conditions in that region, or using existing data if available, and performing the appropriate machine-learning techniques.

In the absence of site-specific measurements, different salinity thresholds for estimating high versus low CH_4 emissions from tidal wetlands have been proposed and are widely cited in the scientific literature. Poffenbarger et al. (2011) proposed a salinity threshold of 18 ppt above which "the methane emitted by a tidal marsh will be less (in CO_2 equivalent units) than the carbon dioxide sequestered as soil carbon in most (95%) tidal marshes." The IPCC Wetland 2013 Supplement (2014) in their Tier 1 emission factors also proposed an 18 ppt salinity threshold, where sites > 18 ppt have no CH_4 emissions and sites < 18 ppt have emissions of 19.4 g CH_4 m^{-2} yr^{-1}. No rationale for this threshold is given in the IPCC Supplement, but Poffenbarger et al. (2011), among others, were cited as criteria. Arias-Ortiz et al. (2024) in a recent synthesis of tidal wetland CH_4 fluxes from the conterminous U.S. (that included data from PNW tidal wetlands reported in Schultz et al. (2023)), suggested more refined IPCC Tier 1 CH_4 emissions factors based upon salinity, elevation class, and average annual daily maximum air temperature (MATmax). Fresh/oligohaline sites and mesohaline sites in low and mid elevation classes and mesohaline sites with MATmax > 19 °C had consequential CH_4 emissions (mean > 21.5 g CH_4 m^{-2} yr-1) . They suggested a cut-off of 21 $\underline{+}$ 2 ppt for consequential CH_4 emissions in tidal wetlands (Arias-Ortiz et al., 2024). However, this synthesis did not consider CH_4 fluxes in the context of the radiative balance of a site in setting thresholds, in contrast to Poffenbarger et al. (2011).

Our data suggest that the salinity threshold of IPCC (2014) would over- or underestimate emissions for many estuarine wetlands in the PNW depending on their salinity and tidal elevation. Our results are in general agreement with Arias-Ortiz et al. (2024). The MATmax of our sites range between 14 and 16 °C (Appendix S1: Table S1), putting our mesohaline sites in the lower tier of CH_4 emissions according to Arias-Ortiz et al. (2024). Correspondingly, we found emissions exceeding 10 g CH_4 m^{-2} yr^{-1} only at salinities below 2-3 ppt (Fig. 8). Our fresh/oligohaline reference marshes and tidal forest sites were mostly high elevation sites relative to tides (Appendix S1: Table S1), and they also tended to have low CH_4 emissions (reference swamp and reference marsh mean = 0.6 and 9.0 g CH_4 m^{-2} yr^{-1}, respectively, Appendix S1; Table S5). We address CH_4 fluxes in the context of the radiative balance of tidal wetlands, similar to Poffenbarger et al. (2011), below.

We plan to compare the effects of CH_4 fluxes versus soil carbon sequestration on the radiative balance of many of these research sites in a future publication, but we can gain perspective here by comparing the average soil carbon accumulation rate for brackish and salt marshes on the Pacific coast of North America, 634 g CO_2 eq m^{-2} yr^{-1} (2 SE = 337; Windham-Myers et al., 2018). We found CH_4 emissions at > 2 ppt salinity to range from 0.5 to 9.6 g CH_4 m^{-2} yr^{-1} (Fig. 8), which equates to 44 to 922 g CO_2 eq m^{-2} yr^{-1} (2 SE = 86) using a 20-year sustained-flux global warming potential (SGWP) and from 21 to 432 g CO_2 eq m^{-2} yr^{-1} (2 SE = 40) with a 100 yr SGWP (Neubauer and Megonigal, 2015). Thus, this preliminary analysis suggests that the radiative balance of brackish and saline wetlands over 2 ppt in the PNW is generally positive (i.e., cooling) with a 100 yr SGWP but is more site-specific with a 20 yr SGWP. Nonetheless, the operative word above for the 100 yr SGWP is "generally" given the large variation in both soil carbon accumulation rates and CH_4 fluxes. Thus, we suggest that CH_4 fluxes be considered in the climate balances of all PNW estuarine wetlands regardless of salinity when weighing the climate effects of management actions. *Most* PNW estuarine wetlands with a salinity > 2 ppt will have a net cooling radiative balance with a 100 yr SGWP, but the substantial effect of CH_4 fluxes on the radiative balance is essential to consider if a quantitative analysis of the climate benefits of management actions is a goal. Our results clearly show that IPCC default values for CH_4 fluxes are inappropriate in PNW estuarine wetlands.

Based upon the current analysis, we can make some preliminary best-management practice suggestions for the PNW. Given the very high CH_4 fluxes we observed in some diked wet pasture sites, restoration focused on former tidal wetlands with a high water table may have the greatest impact on reducing GHG emissions, provided that restoration actions lower the water table. A beneficial change in emissions will be particularly large if the site converts from a freshwater or oligohaline state to a more saline condition upon restoration. We expect less climate benefit from restoring dry pastures, although many other ecosystem benefits will accrue in such sites. According to our findings, restored marshes are second only to wet pastures in CH_4 emissions, but we suggest that as sites evolve (Simenstad and Thom, 1996), they will have lower CH_4 emissions as they approach greater functional recovery.

Restored tidal wetland sites in the PNW are typically at a lower elevation than reference sites because of past subsidence (Frenkel and Morlan, 1991). If fill is used in the restoration process to create a higher wetland, then lower CH_4 fluxes would be expected regardless of the site's salinity. Excavation to restore tidal channel networks can result in material useful for creating higher elevation wetland areas within a site (Diefenderfer et al., 2018b), though such an approach presents permitting, ecological, and logistical challenges (Piercy et al., 2023). Effective tidal drainage from a restored site, such as the construction of a channel network of sufficient density, could also reduce CH_4 fluxes by lowering the water table during low tide periods. Over time, lower elevation restored marshes accrete sediment and gain elevation, but it may take many decades for them to reach similar elevations to their reference counterparts (Thom, 1992; Cornu and Sadro, 2002). Typical rates of reference marsh accretion in the PNW range from 0.8 to 4.1

mm yr^{-1} across a wide range of fluvial suspended sediment load (Thom, 1992; Peck et al., 2020). Yet accretion rates up to an order of magnitude higher have been reported in some PNW estuaries, including in reference and restored sites in the Columbia Estuary (7-24 mm yr^{-1}; Diefenderfer et al., 2008; Diefenderfer et al., 2021), suggesting that some restoration sites may be capable of reaching reference wetland elevations more quickly which may lead to reductions in CH_4 emissions.

Another recommended focus of restoration in PNW estuaries is tidal swamps, which were once widespread in the PNW with greater extent than marshes but are now almost completely lost (Brophy, 2019). Swamp restoration may have a substantial climate benefit in fresh-oligohaline conditions where restoration of marshes may yield less carbon accumulation and long-term storage. Forested tidal swamps tend to require a higher tidal elevation for persistence (Brophy et al., 2011), but the high carbon stocks in both tree biomass and soils in the relatively few extant tidal swamps (Kauffman et al., 2020) suggest they have among the highest capacities for total ecosystem carbon stocks accumulation globally of any blue carbon ecosystem.

ACKNOWLEDGMENTS

This research is a product of the Pacific Northwest Blue Carbon Working Group and was funded by the Effects of Sea-level Rise program at NOAA-NCCOS (grant NA19NOS4780176) and the National Estuarine Research Reserve System's Science Collaborative program (grant NA19NOS4190058). We are grateful to the many land owners and managers who facilitated access to study sites, including the Washington Department of Fish and Wildlife, Columbia Land

Trust, South Slough NERR, Padilla Bay NERR, National Park Service, Port of Astoria, City of Coos Bay, Warrenton Public Works, and Sause Bros., Inc. The Pacific Northwest National Laboratory kindly loaned a LI-COR GHG analyzer used for many of the measurements in this study and the Institute for Applied Ecology and US EPA kindly loaned some of the data loggers used for groundwater data collection.

CONFLICTS OF INTEREST STATEMENT

The authors declare that they have no conflicts of interest concerning this publication.

AUTHOR CONTRIBUTIONS

TW conducted field work, led analyses, and led the first draft of the paper. CJ and SB helped secure funding and design the study, assisted with field work and analyses, and helped write the paper. MM and MS conducted field work and edited the paper. MN assisted with field work. CC, AB, and JA helped secure funding, design the study, conduct field work, and edit the paper. LB and HD helped secure funding, design the study, and edit the paper.

LITERATURE CITED

Al-Haj AN, Fulweiler RW. 2020. A synthesis of methane emissions from shallow vegetated coastal ecosystems. Global Change Biology 26:2988-3005.

Arias-Ortiz A, Wolfe J, Bridgham SD, Knox S, McNicol G, Needelman BA, Shahan J, Stuart-Haëntjens EJ, Windham-Myers L, Oikawa P, Baldocchi DD, Caplan JS, Capooci M, Czapla KM, Derby RK, Diefenderfer HL, Forbrich I, Groseclose G, Keller JK, Kelley C, Keshtna AE, Kleiner HS, Krauss KW, Lane RR, Mack S, Mosemann-Valtierra S, Mozdzer T, Mueller P, Neubauer SC, Noyce G, Schäfer KVR, Sanders-DeMott R, Schutte C, Vargas R, Weston NB, Wilson B, Megonigal JP, Holmquist JR. 2024. Methane fluxes in tidal marshes of the conterminous United States. Global Change Biology 30: e17462. https://doi.org/10.1111/gcb.17462.

Baggs EM. 2011. Soil microbial sources of nitrous oxide: recent advances in knowledge, emerging challenges and future direction. Current Opinion in Environmental Sustainability 3:321-327.

Borde AB, Diefenderfer HL, Cullinan VI, Zimmerman SA, Thom RM. 2020. Ecohydrology of wetland plant communities along an estuarine to tidal river gradient. Ecosphere 11:e03185.

Bridgham SD, Cadillo-Quiroz H, Keller JK, Zhuang Q. 2013. Methane emissions from wetlands: biogeochemical, microbial, and modeling perspectives from local to global scales. Global Change Biology 19:1325-1346.

Bridgham SD, Megonigal JP, Keller JK, Bliss NB, Trettin C. 2006. The carbon balance of North American wetlands. Wetlands 26:889-916.

Brophy L. 2019. Comparing historical losses of forested, scrub-shrub, and emergent tidal wetlands on the Oregon coast, USA: A paradigm shift for estuary restoration and conservation. Estuary Technical Group, Institute for Applied Ecology, Corvallis, OR.

Brophy LS, Cornu CE, Adamus PR, Christy JA, Gray A, MacClellan MA, Doumbia JA, Tully RL. 2011. New tools for tidal wetland restoration: Development of a reference conditions database and a temperature sensor method for detecting tidal inundation in least-disturbed tidal wetlands of Oregon, USA. Report to the Cooperative Institute for Coastal and Estuarine Environmental Technology (CICEET), Durham, NH. https://doi.org/10.13140/RG.2.2.12864.87046

Brophy LS, Greene CM, Hare VC, Holycross B, Lanier A, Heady WN, O'Connor K, Imaki H, Haddad T, Dana R. 2019. Insights into estuary habitat loss in the western United States using a new method for mapping maximum extent of tidal wetlands. PLoS ONE 14:e0218558.

Bubier JL, Moore TR, Juggins S. 1995. Predicting methane emission from bryophyte distribution in northern Canadian peatlands. Ecology 76:677-693.

Butterbach-Bahl K, Baggs EM, Dannenmann M, Kiese R, Zechmeister-Boltenstern S. 2013. Nitrous oxide emissions from soils: how well do we understand the processes and their controls? Philos Trans R Soc Lond B Biol Sci 368:20130122.

Cade BS, Noon BR. 2003. A gentle introduction to quantile regression for ecologists. Frontiers Ecology Environment 1:412-420.

Capooci M, Vargas R. 2022. Trace gas fluxes from tidal salt marsh soils: Implications for carbon-sulfur biogeochemistry. Biogeosciences 19:4655-4670.

Chmura GL, Anisfeld SC, Cahoon DR, Lynch JC. 2003. Global carbon sequestration in tidal, saline wetland soils. Global Biogeochemcial Cycles 17:1111.

Cornu CE, Sadro S. 2002. Physical and functional responses to experimental marsh surfrace elevation manipulation in Coos Bay's South Slough. Restoration Ecology 10:474-486.

David AT, Ellings CS, Woo I, Simenstad CA, Takekawa JY, Turner KL, Smith AL. 2014. Foraging and growth potential of juvenile Chinook salmon after tidal restoration of a large river delta. Transactions of the American Fisheries Society 143:1515-1529.

Dias ATC, Hoorens B, Logtestijn RSP, Vermaat JE, Aerts R. 2010. Plant species composition can be used as a proxy to predict methane emissions in peatland ecosystems after land-use changes. Ecosystems 13:526-538.

Diefenderfer HL, Borde AB, Cullinan VI. 2021. Floodplain wetland channel planform, cross-sectional morphology, and sediment characteristics along an estuarine to tidal river gradient. Journal of Geophysical Research: Earth Surface 126:e2019JF005391.

Diefenderfer HL, Coleman AM, Borde AB, Sinks IA. 2008. Hydraulic geometry and microtopography of tidal freshwater forested wetlands and implications for restoration, Columbia River, USA. Ecohydrology & Hydrobiology 8:339-361.

Diefenderfer, H. L., V. I. Cullinan, A. B. Borde, C. M. Gunn, and R. M. Thom. 2018a. High-Frequency Greenhouse Gas Flux Measurement System Detects Winter Storm Surge Effects on Salt Marsh. Global Change Biology 24: 5961–71. https://doi.org/10.1111/gcb.14430

Diefenderfer HL, Sinks IA, Zimmerman SA, Cullinan VI, Borde AB. 2018b. Designing topographic heterogeneity for tidal wetland restoration. Ecological Engineering 123:212-225.

Frenkel RE, Morlan JC. 1991. Can we restore our salt marshes? Lessons from the Salmon River, Oregon. The Northwest Environmental Journal 7:119-135.

Greenwell, B. Boehmke, J. Cunningham, and Developers GBM. 2022. gbm: Generalized Boosted Regression Models." R Package Version 2.1.8.1.

Hemes KS, Chamberlain SD, Eichelmann E, Knox SH, Baldocchi DD. 2018. A biogeochemical compromise: The high methane cost of sequestering carbon in restored wetlands. Geophysical Research Letters 45:6081-6091.

Himes-Cornell A, Pendelton L, Atiyah P. 2018. Valuing ecosystem services from blue forests: A systematic review of the valuation of salt marshes, seagrass beds and mangrove forests. Ecosystem Services 30:36-48.

Hopkinson CS, Wei-Jun Cai, and Xinping Hu. 2012. Carbon sequestration in wetland dominated coastal systems—a global sink of rapidly diminishing magnitude. Current Opinion in Environmental Sustainability 4:186–94. https://doi.org/10.1016/j.cosust.2012.03.005.

IPCC. 2014. 2013 Supplement to the 2006 IPCC Guidelines for National Greenhouse Gas Inventories: Wetlands. IPCC, Switzerland.

Janousek, C., T. Williams, M. McKeon, S. D. Bridgham, C. Cornu, H. Diefenderfer, A. Borde, M. Norwood, J. Apple, and L. Brophy. 2025. Dataset: Fluxes of Carbon Dioxide, Methane, and Nitrous Oxide and Associated Environmental Data from Estuarine Wetlands in the Pacific Northwest, USA. Smithsonian Environmental Research Center. https://doi.org/10.25573/serc.27161883.v1.

Janousek CN, Folger CL. 2014. Variation in tidal wetland plant diversity and composition within and among coastal estuaries: Assessing the relative importance of environmental gradients. Journal of Vegetation Science 25:534-545.

Johannessen SC, Christian JR. 2023. Why blue carbon cannot truly offset fossil fuel emissions. Communications Earth & Environment 4:411.

Kauffman JB, Giovanonni L, Kelly J, Dunstan N, Borde A, Diefenderfer H, Cornu C, Janousek C, Apple J, Brophy L. 2020. Total ecosystem carbon stocks at the marine-terrestrial interface: Blue carbon of the Pacific Northwest coast, United States. Global Change Biology 26:5679-5692.

Kelleway JJ, Serrano O, Baldock JA, Burgess R, Cannard T, Lavery PS, Lovelock CE, et al. 2020. A National Approach to Greenhouse Gas Abatement through Blue Carbon Management. Global Environmental Change 63: 102083. https://doi.org/10.1016/J.GLOENVCHA.2020.102083.

Koenker, R. 2005. Quantile Regression. Econometric Society Monographs. Cambridge, UK: Cambridge University Press.

Kuhn, M. 2022. caret: Classification and Regression Training. R package version 6.0-93.

Laanbroek HJ. 2010. Methane emission from natural wetlands: interplay between emergent macrophytes and soil microbial processes. A mini-review. Annals of Botany 105:141-153.

Lawson T, Blatt MR. 2014. Stomatal size, speed, and responsiveness impact on photosynthesis and water use efficiency. Plant Physiology 164:1556-1570.

Marcoe, K, Pilson, S. 2017. Habitat changes in the lower Columbia River estuary, 1870-2009. Journal of Coastal Conservation 21:505-525.

McLeod E, Chmura GL, Bouillon S, Salm R, Björk M, Duarte CM, Lovelock CE, Schlesinger WH, Silliman BR. 2011. A blueprint for blue carbon: Toward an improved understanding of the role of vegetated coastal habitats in sequestering CO2." Frontiers in Ecology and the Environment 9: 552–60. https://doi.org/10.1890/110004.

Megonigal JP, Hines ME, Visscher PT. 2004. Anaerobic metabolism: linkages to trace gases and aerobic processes. Pages 317-424 in W. H. Schlesinger, editor. Biogeochemistry. Elsevier-Pergamon, Oxford, UK.

Moseman-Valtierra, S. 2012. Reconsidering climatic roles of marshes: Are they sinks or sources of greenhouse gases? Pages 1-48 in D. C. Abreu and S. L. de Borbón, editors. Marshes: Ecology, Management and Conservation. Nova Science Publishers, Inc., New York.

Neubauer SC, Megonigal JP. 2015. Moving beyond global warming potentials to quantify the climatic role of ecosystems. Ecosystems 18:1000-1013.

NOAA 2003. Computational techniques for tidal datums handbook. Silver Springs, MD: NOAA Special Publication NOS CO-OPS 2.

O'Connor JJ, Fest BJ, Sievers M, Swearer SE. 2020. Impacts of land management practices on blue carbon stocks and greenhouse fluxes in coastal ecosystems--A meta-analysis. 26:1354-1366.

Oksanen J. 2015. Multivariate analysis of ecological communities in R: vegan tutorial.

Oksanen J, Simpson GL, Blanchet G, Kindt R, Legendre P, Minchin PR, O'Hara RB, Solymos P, Stevens MHH, Szoecs E, Wagner H, Barbour M, Bedward M, Bolker B, Borcard D, Carvalho G, Chirico M, Da Cacerces M, Durand S, Evangelists HBA, FitzJohn R, Friendly M, Furneaux B, Hannigan G, Hill MO, Lahti L, McGlinn D, Ouellette M-H, Cunha ER, Smith T, Stier A, Ter Braak CJF, Weedon J. 2022. Vegan: Community Ecology Package. R package v. 2.6-2.

Peck EK, Wheatcroft RA, Brophy LS. 2020. Controls on sediment accretion and blue carbon burial in tidal saline wetlands: Insights from the Oregon coast, USA. JGR Biogeosciences 125:e2019JG005464.

Piercy, C.D., T. L. Welp, and R. Mohan, R., 2023. Guidelines for how to Approach Thin Layer Placement Projects. Vicksburg, MS: US Army Engineer Research and Development Center, Environmental Laboratory.

Poffenbarger HJ, Needelman BA, Megonigal JP. 2011. Salinity Influence on Methane Emissions from Tidal Marshes. Wetlands 31: 831–42. https://doi.org/10.1007/S13157-011-0197-0/FIGURES/3.

Poppe KL, Rybczyk JM. 2021. Tidal marsh restoration enhances sediment accretion and carbon accumulation in the Stillaguamish River estuary, Washington. PLoS ONE 16:e0257244

R Core Team (2020). R: A language and environment for statistical computing. R Foundation for Statistical Computing, Vienna, Austria. URL https://www.R-project.org/.

Rosentreter JA, Al-Haj AN, Fulweiler RW, Williamson P. 2021. Methane and nitrous oxide emissions complicate coastal blue carbon assessments. Global Biogeochemical Cycles 35. https://doi.org/10.1029/2020GB006858.

Rosentreter JA, Laruelle GG, Bange HW, Bianchi TS, Busecke JJM, Cai W-J, Eyre BD, Forbrich I, Kwon EY, Maavara T, Moosdorf N, Najjar RG, Sarma VVSS, Van Dam B, Regnier P. 2023. Coastal vegetation and estuaries are collectively a greenhouse gas sink. Nature Climate Change 13:579-587.

RoyChowdhury T, Bramer L, Hoyt DW, Kim YM, Metz TO, McCue LA, Diefenderfer HL, Jansson JK, Bailey V. 2018. Temporal dynamics of CO_2 and CH_4 loss potentials in response to rapid hydrological shifts in tidal freshwater wetland soils. Ecological Engineering 114:104-14.

Sanders-Demott R, Eagle MJ, Kroeger KD, Wang F, Brooks TW, O'Keefe Suttles JA, Nick SK, Mann AG, Tang J. 2022 Impoundment increases methane emissions in Phragmites-invaded coastal wetlands. Global Change Biology 28:4539-4557. https://doi.org/10.1111/GCB.16217.

Schultz MA, Janousek CN, Brophy LS, Schmitt J, Bridgham SD. 2023. How management interacts with environmental drivers to control greenhouse gas fluxes from Pacific Northwest tidal wetlands. Biogeochemistry 165:165-190.

Silva LCR, Wood MC, Johnson BR, Coughlan MR, Brinton H, McGuire K, Bridgham SD. 2022. A generalizable framework for enhanced natural climate solutions. Plant and Soil 479:3-24.

Simenstad CA, Thom RM. 1996. Functional equivalency trajectories of the restored Gog-Le-Hi-Te estuarine wetland. Ecological Applications 6:38-56.

Swanson KM, Drexler JZ, Schoellhamer DH, Thorne KM, Casazza ML, Overton CT, Callaway JC, Takekawa JY. 2014. Wetland accretion rate model of ecosystem resilience (WARMER) and its application to habitat sustainability for endangered species in the San Francisco estuary. Estuaries and Coasts 37:476-492.

Tan L, Ge Z, Zhou X, Li S, Li X. 2020. Conversion of coastal wetlands, riparian wetlands, and peatlands increases greenhouse gas emissions: A global meta-analysis. Global Change Biology 26:1638-1653.

Thom RM. 1992. Accretion rates of low intertidal salt marshes in the Pacific Northwest. Wetlands 12: 147-156.

Vroom RJE, van den Berg M, Pangala SR, van der Scheer OE, Sorrell BK. 2022. Physiological processes affecting methane transport by wetland vegetation – A review. Aquatic Botany 182

Watson EB, Byrne R. 2009. Abundance and diversity of tidal marsh plants along the salinity gradient of the San Francisco Estuary: Implications for global change ecology. Plant Ecology 205:113-128.

Windham-Myers, L., W.-J. Cai, S. R. Alin, A. Andersson, J. Crosswell, K. H. Dunton, J. M. Hernandez-Ayon, M. Herrmann, A. L. Hinson, C. S. Hopkinson, J. Howard, X. Hu, S. H. Knox, K. Kroeger, D. Lagomasino, P. Megonigal, R. G. Najjar, M.-L. Paulsen, D. Peteet, E. Pidgeon, K. V. R. Schäfer, M. Tzortziou, Z. A. Wang, and E. B. Watson. 2018. Chapter 15:

Tidal wetlands and estuaries. Pages 596-648 in N. Cavallaro, G. Shrestha, R. Birdsey, M. A. Mayes, R. G. Najjar, S. C. Reed, P. Romero-Lankao, and Z. Zhu, editors. Second State of the Carbon Cycle Report (SOCCR2): A Sustained Assessment Report, U.S. Global Change Research Program, Washington, DC.

Wu Q, Ye R, Bridgham SD, Jin Q. 2021. Limitations of the Q10 coefficient for quantifying temperature sensitivity of anaerobic organic matter decomposition: A modeling based assessment. Journal of Geophysical Research: Biogeosciences 126:e2021JG006264.

Yuan, K., Q. Zhu, F. Li, W. J. Riley, M. Torn, H. Chu, G. McNicol, M. Chen, S. Knox, K. Delwiche, H. Wu, D. Baldocchi, H. Ma, A. R. Desai, J. Chen, T. Sachs, M. Ueyama, O. Sonnentag, M. Helbig, E.-S. Tuittila, G. Jurasinski, F. Koebsch, D. Campbell, H. P. Schmid, A. Lohila, M. Goeckede, M. B. Nilsson, T. Friborg, J. Jansen, D. Zona, E. Euskirchen, E. J. Ward, G. Bohrer, Z. Jin, L. Liu, H. Iwata, J. Goodrich, and R. Jackson. 2022. Causality guided machine learning model on wetland CH4 emissions across global wetlands. Agricultural and Forest Meteorology 324.

Zhang Z, Poulter B, Feldman AF, Ying Q, Ciais P, Peng S, Li X. 2023. Recent intensification of wetland methane feedback. Nature Climate Change 13:430-433.

Ecological Applications

Methane and nitrous oxide fluxes from reference, restored, and disturbed estuarine wetlands in Pacific Northwest, USA

Trevor Williams, Christopher N. Janousek, Maggie A. McKeon, Heida L. Diefenderfer, Craig E. Cornu, Amy B. Borde, Jude Apple, Laura S. Brophy, Matthew Norwood, Matthew A. Schultz, Scott D. Bridgham

Appendix S1

TABLE S1. List of study sites, estuary, wetland type, geographic location, average annual groundwater salinity at the site (in ppt), elevation, and average annual daily maximum air temperature (°C, MAXtemp). Salinities were determined from groundwater logger time series unless otherwise noted, and MAXtemp is the 1991-2020 annual mean maximum temperature from the PRISM climate model (http://www.prism.oregonstate.edu). Elevations are site means (±SD) of tide-range standardized elevations (z*) at the six chamber locations per site (n = 4 at Milltown Island swamp).

Site	**Estuary (state)**	**Wetland type**	**Latitude**	**Longitude**	**Salinity**	**Elevation**	**MAXtemp**
Wasson Creek upper pasture	Coos (OR)	Dry pasture	43.27173	-124.32409	0.1*	2.39 ± 0.04	15.6
Wasson Creek lower pasture	Coos (OR)	Dry pasture	43.27067	-124.32174	0.1*	1.46 ± 0.09	15.8
Winchester Creek swamp	Coos (OR)	Tidal swamp	43.26943	-124.32101	2.1	1.15 ± 0.04	15.8
Fredrickson south marsh	Coos (OR)	Reference marsh	43.27239	-124.31885	10.7	1.12 ± 0.04	15.6
Fredrickson restored marsh	Coos (OR)	Reference marsh	43.27481	-124.32033	16.1	0.99 ± 0.06	15.6
Kunz restored marsh (high cell)	Coos (OR)	Restored marsh	43.28057	-124.31885	19.7	0.97 ± 0.05	15.6
Kunz restored marsh (low cell)	Coos (OR)	Restored marsh	43.28171	-124.31957	22.9	0.46 ± 0.12	15.6
Danger Pt marsh	Coos (OR)	Reference marsh	43.28335	-124.32342	9.0	0.82 ± 0.20	15.6
Metcalf marsh	Coos (OR)	Reference marsh	43.33526	-124.32829	18.7	0.89 ± 0.15	14.9
Millicoma marsh	Coos (OR)	Reference marsh	43.36810	-124.18532	16.9	1.02 ± 0.03	15.6
Millicoma restored marsh	Coos (OR)	Restored marsh	43.36734	-124.18500	16.8	1.28 ± 0.03	15.6
Sause pasture	Coos (OR)	Dry pasture	43.36835	-124.18409	1.1	0.59 ± 0.02	15.6
Secret River marsh	Columbia (WA)	Reference marsh	46.30497	-123.69242	0.1*	0.41 ± 0.03	14.1
Secret River swamp	Columbia (WA)	Tidal swamp	46.30766	-123.68992	0.1*	1.14 ± 0.11	14.1
Alder Road pasture	Columbia (WA)	Wet pasture	46.31446	-123.68349	0.3*	0.51 ± 0.03	15.3
Kandoll Farm marsh	Columbia (WA)	Restored marsh	46.32616	-123.65401	0.1*	0.52 ± 0.08	15.3
Seal Slough swamp	Columbia (WA)	Tidal swamp	46.32647	-123.65992	0.1*	0.92 ± 0.08	15.3
Mouth Lewis Clark Riv marsh	Columbia (OR)	Reference marsh	46.15775	-123.86157	3.3	0.70 ± 0.03	14.0
South Clatsop Slough marsh	Columbia (OR)	Restored marsh	46.12910	-123.87931	1.7	0.73 ± 0.09	14.7
Johns River polyhaline marsh	Grays Harbor (WA)	Reference marsh	46.90081	-123.99240	16.5	1.03 ± 0.01	13.6
Johns River mesohaline marsh	Grays Harbor (WA)	Reference marsh	46.89158	-123.98729	7.2	1.32 ± 0.03	14.3
Johns River south pasture	Grays Harbor (WA)	Wet pasture	46.89342	-123.98842	0.4	1.18 ± 0.06	14.3
Johns River north pasture	Grays Harbor (WA)	Dry pasture	46.89867	-123.98821	0.3	0.98 ± 0.05	13.6
Johns River oligohaline marsh	Grays Harbor (WA)	Reference marsh	46.88344	-123.96458	5.0	1.18 ± 0.06	14.6
Johns River restored marsh	Grays Harbor (WA)	Restored marsh	46.90513	-123.99071	17.9	0.70 ± 0.10	13.6
Johns River swamp	Grays Harbor (WA)	Tidal swamp	46.88292	-123.96576	3.9	1.15 ± 0.05	14.6
Milltown Island oligohaline marsh	Skagit (WA)	Reference marsh	48.30145	-122.35995	1.3	0.80 ± 0.03	14.4
Milltown Island restored marsh	Skagit (WA)	Restored marsh	48.31730	-122.34848	0.7	1.03 ± 0.04	15.0
Milltown Island swamp	Skagit (WA)	Tidal swamp	48.31744	-122.34747	0.2	1.37 ± 0.05	15.0
Fir Island marsh	Skagit (WA)	Reference marsh	48.33332	-122.41500	7.4	0.83 ± 0.03	14.4
Fir Island restored marsh	Skagit (WA)	Restored marsh	48.33520	-122.41038	7.1	0.38 ± 0.05	14.4
Padilla Bay agricultural field	Padilla (WA)	Dry pasture	48.46369	-122.46956	0.2	0.08 ± 0.04	14.8
Padilla Bay wet pasture	Padilla (WA)	Wet pasture	48.45705	-122.46960	3.5	-0.46 ± 0.11	14.8
Big Indian Slough marsh	Padilla (WA)	Reference marsh	48.45392	-122.47308	27.2	0.86 ± 0.02	14.8

*Salinity from occasional spot measurements made with a hand-held meter.

TABLE S2. Relative influence (%) of eight environmental factors on point measurements of CH_4 and N_2O fluxes in BRT models.

Factor	**CH_4 model**	**N_2O model**
Elevation (z*)	21.1	15.9
Salinity	18.3	12.2
Water-table level	16.0	19.3
Wetland type	12.1	21.8
Soil temperature	9.4	7.3
pH	8.4	8.3
Air temperature	7.7	9.2
Groundwater temperature	6.9	5.9

TABLE S3. List of common and indicator plant species used in the NMDS analysis of species composition and CH_4 and N_2O fluxes.

Species	**Common name**	**Code**
Agrostis stolonifera	Creeping bentgrass	AgrSto
Carex lyngbyei	Lyngbye’s sedge	CarLyn
Carex obnupta	Slough sedge	CarObn
Distichlis spicata	Salt grass	DisSpi
Holcus lanatus	Velvetgrass	HolLan
Jaumea carnosa	Fleshy jaumea	JauCar
Juncus balticus	Baltic rush	JunBal
Lysichiton americanum	Skunk cabbage	LysAme
Bryophytes	Mosses	Moss
Oenanthe sarmentosa	Water parsley	OenSar
Phalaris arundinaceus	Reed canarygrass	PhaAru
Potentilla anserina	Pacific silverweed	PotAns
Sagittaria latifolia	Wapato	SagLat
Salicornia pacifica	Pickleweed	SalPac
Schoenoplectus spp.	Tule	Sch

TABLE S4. Summary statistics of point measurements of CH_4 fluxes by wetland type in PNW estuaries. Data summaries combine all sampling dates and sites. Positive values indicate a net flux to the atmosphere.

CH_4 flux (nmol m^{-2} min^{-1})						
Wetland class	**N**	**Mean**	**SE**	**Median**	**Max**	**Min**
Reference swamp	202	266	92	0	16,004	-131
Reference marsh	491	418	56	17	13,190	-99
Restored marsh	399	1824	446	243	130,971	-130
Wet pasture	102	8010	2505	7	197,977	-31
Dry pasture	218	20	17	0	2,983	-285

TABLE S5. Modeled annual CH_4 fluxes for wetland classes subset within salinity classes from the BRT model. Included are all sites from this study, and three additional reference marshes and six additional restored marshes in Tillamook Bay, OR reported by Schulz et al. (2023).

	Predicted CH_4 flux (g CH_4 m^{-2} yr^{-1})					
Wetland class	**N**	**Mean**	**SE**	**Median**	**Max**	**Min**
Fresh + oligohaline (0-5 ppt)						
Reference swamp	5	0.56	0.15	0.58	0.96	0.08
Reference marsh	5	9.01	6.41	2.88	34.61	1.15
Restored marsh	4	124.41	99.79	37.74	420.03	2.13
Wet pasture	2	55.03	51.43	55.03	106.46	3.60
Dry pasture	5	0.21	0.84	0.14	3.26	-1.39
Mesohaline (5-18 ppt)						
Reference marsh	8	2.25	0.64	1.64	6.15	0.75
Restored marsh	9	3.53	0.91	3.66	9.61	0.46
Wet pasture	1	1.70	NA	1.70	NA	NA
Polyhaline (18-30 ppt)						
Reference marsh	2	1.81	0.06	1.81	1.87	1.74
Restored marsh	2	7.53	0.84	7.53	8.37	6.69

TABLE S6. Summary of linear relationships between point measurements of N_2O fluxes and individual environmental drivers in PNW tidal wetlands.

Environmental driver	**Model fits to mean fluxes**		
	Coefficient	**R^2**	**P**
Salinity	0.003	-0.001	0.45
Water -table level	-0.075	0.030	>0.001
Groundwater pH	-0.062	0.004	0.10
Groundwater temperature	0.002	-0.003	0.63
Wetland elevation	0.065	-0.00009	0.33
Soil temperature	-0.010	-0.004	0.73
Air temperature	-0.008	-0.0004	0.37

TABLE S7. Summary of point measurements of N_2O fluxes by wetland type in Pacific Northwest estuaries.

N_2O fluxes (nmol m^{-2} min^{-1})						
Wetland class	**N**	**Mean**	**SD**	**Median**	**Max**	**Min**
Reference swamp	78	1.3	5.4	0	20	-12
Reference marsh	143	-0.36	9.3	0	49	-60
Restored marsh	149	0.061	5.2	0	30	-28
Wet pasture	24	1.3	6.4	0	31	-0
Dry pasture	75	7.8	18	0	93	-18

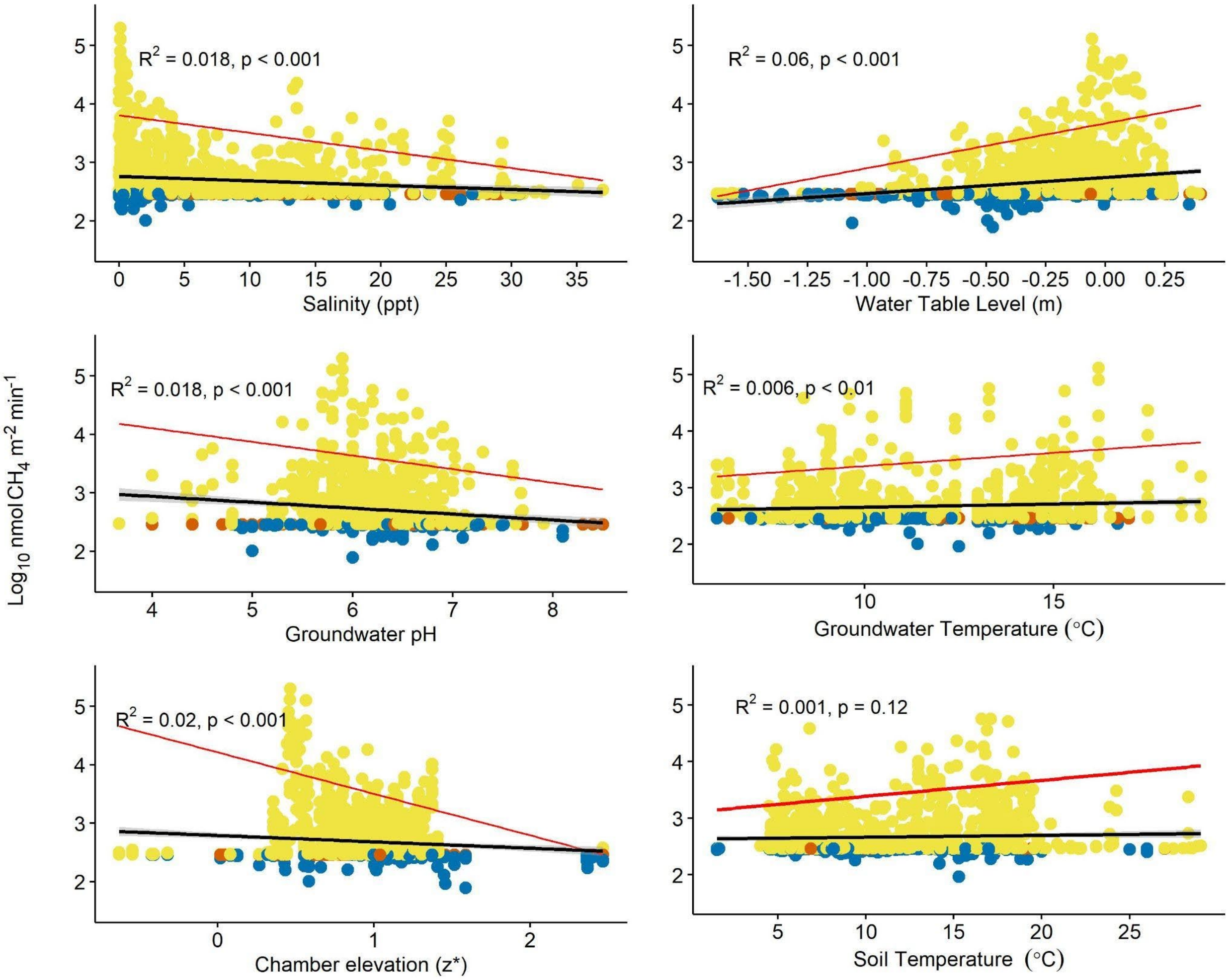

FIG. S1. Scatter plots showing relationships between point measurements of $\log_{10}$ CH_4 flux and select environmental drivers. Yellow points represent net emissions to the atmosphere, blue points represent net uptake, and red points represent no change. Gray envelopes around black regression lines represent 95% confidence intervals (with R^2 and P statistics); red lines indicate 95% quantile regressions.

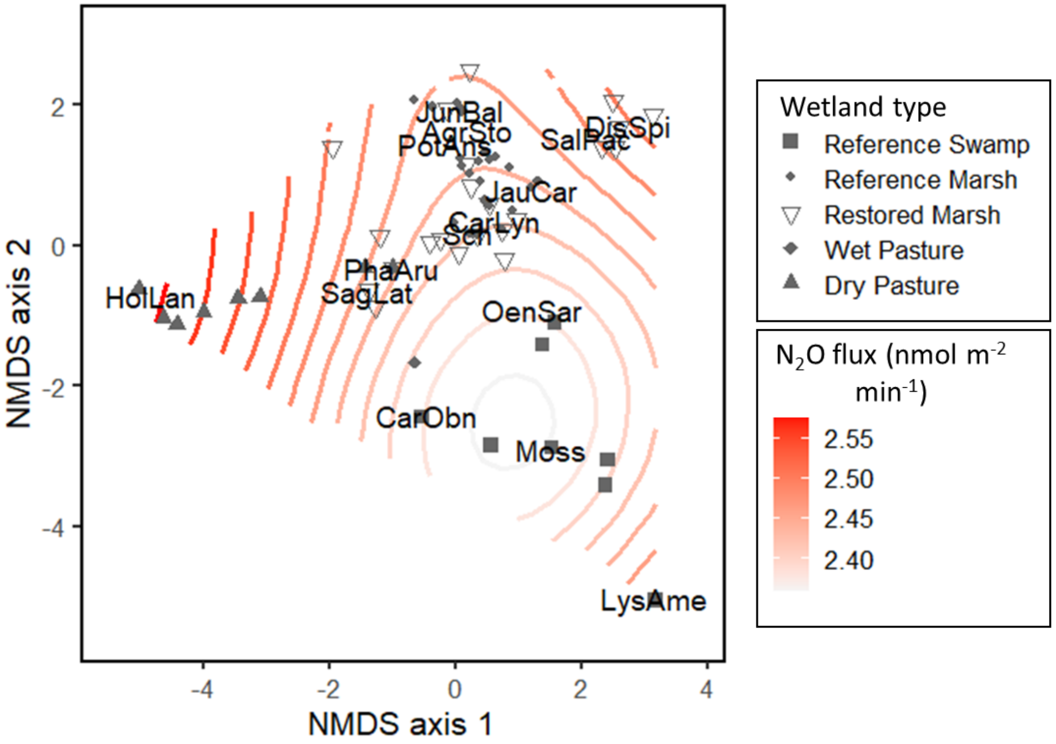

FIG S2. Relationship between plant species composition in two dimensional NMDS space and point measurements of N_2O fluxes (nmol m^{-2} min^{-1}) during summer sampling in the Coos and Columbia River estuaries. Individual chambers are indicated by points. The centroids of common and indicator species are given by six letter codes as in Table S3. Modeled N_2O fluxes across the species compositional space are indicated by color contours.

References

Schultz, M. A., C. N. Janousek, L. S. Brophy, J. Schmitt, and S. D. Bridgham. 2023. How management interacts with environmental drivers to control greenhouse gas fluxes from Pacific Northwest tidal wetlands. Biogeochemistry 165:165-190.